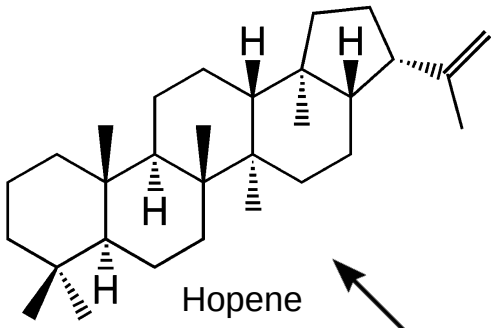

Hopene

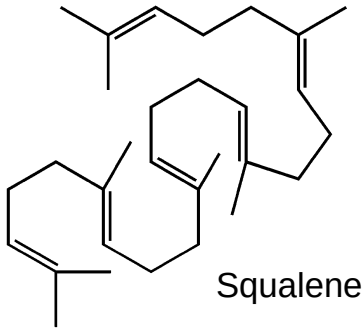

Squalene

Cyclase

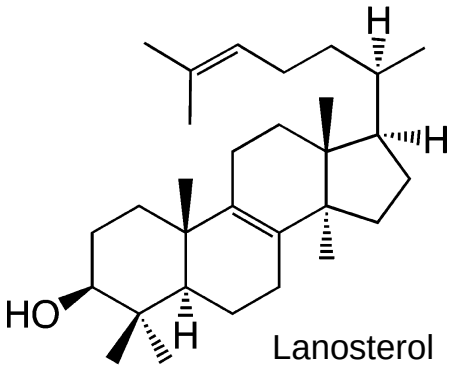

Lanosterol

Enzyme Mechanisms for Polycyclic Triterpene Formation

K. Ulrich Wendt, Georg E. Schulz,* Elias J. Corey, and David R. Liu*

The mechanisms by which triterpene cyclases transform olefins into complex and biologically important polycyclic products have fueled nearly half a century of intense research. Recent chemical and biological studies, together with previous findings, provide intriguing new insights into the enzymatic mechanism of triterpene formation and form a surprisingly detailed picture of these elegant catalysts. It can be concluded that the role of the oxidosqualene cyclases involves protection of the intermediate carbocation against addition of water or deprotonation by base, thereby allowing the shift of the hydride and methyl groups along a thermodynamically and kinetically favorable cascade. Key questions in the areas of structural biology, site-directed mutagenesis, and directed evolution are apparent, now that the first structure of a triterpene cyclase is known.

Keywords: bioorganic chemistry · cyclases · enzymatic catalysis · steroids · structural biology

1. Introduction

For nearly half a century the remarkable enzymatic cyclizations of squalene (**1**) and 2,3-oxidosqualene (**2**; Figure 1) to form polycyclic triterpenes have provided both fascination and challenge in the molecular sciences.[1–10] These polyolefins are stereoselectively cyclized and skeletally rearranged in a single enzyme-catalyzed reaction by a wide range of microorganisms and higher eukaryotes to yield tetracyclic and pentacyclic triterpenoids including hopene (**3**), diplopterol (**4**), tetrahymanol (**5**), lanosterol (**6**), cycloartenol (**7**), and β-amyrin (**8**; Figure 1). These triterpenes in turn serve as the precursors of all hopanoids and steroids, including cholesterol, glucocorticoids, estrogens, androgens, and progesterones. The remarkably powerful and efficient transformation catalyzed by the triterpene cyclases stimulated the interest of pioneering organic chemists nearly a half century ago. [1–9, 11] Their early chemical studies on these enzymes identified the intermediacy of oxidosqualene in steroid biosynthesis and clarified the stereochemical course of the cyclization as well as the 1,2-hydride and methyl group migrations which follow the cyclization.[3–9]

Early studies on triterpene cyclases focused on the use of substrate analogues to define the range of structures which the cyclases can transform and the nature of any resulting products.[9] While these chemical studies have provided useful mechanistic information, more recent research employing molecular and structural biology in conjunction with bioorganic chemistry has yielded a wealth of new data. Taken together, these findings offer surprisingly detailed insights into the complex series of molecular events involved in squalene and oxidosqualene cyclization. Below we review these studies as applied to unraveling the complexities of triterpene cyclization.

2. The Reaction Pathway: Chemical Studies

The formation of tetracyclic or pentacyclic triterpenes from squalene (**1**) or oxidosqualene (**2**) has never been achieved efficiently in purely nonenzymatic experiments, despite numerous attempts to duplicate this powerful one-step enzyme-catalyzed transformation, outlined briefly in Figure 2. The formation of a six-membered ring by intramolecular addition of a carbocation to a carbon–carbon double bond is highly exothermic ($\Delta E = E_{\sigma\text{-CC}} - E_{\pi\text{-CC}} \approx 20$ kcal mol^{-1}) and requires little activation (zero to a few kcal mol^{-1}, depending on solvation).[12] Accordingly, cationic cyclizations of conformationally mobile substrates are difficult to control

[*] Prof. Dr. G. E. Schulz, Dr. K. U. Wendt[+]
Institut für Organische Chemie und Biochemie
Albertstrasse 21, 79104 Freiburg (Germany)
Fax: (+49) 761-203-6161
E-mail: schulz@chemie.uni-freiburg.de
Prof. Dr. D. R. Liu, Prof. Dr. E. J. Corey
Department of Chemistry and Chemical Biology
Harvard University
12 Oxford Street, Cambridge, MA 02138 (USA)
Fax: (+1) 617-496-5688
E-mail: drliu@fas.harvard.edu
[+] Department of Protein Engineering
Genentech Inc.
DNA Way, South San Francisco, CA 94080-4990 (USA)

  1433-7851/00/3916-2813 $ 17.50+.50/0

because numerous reaction modes of low activation energy compete effectively and lead to a variety of products.

2.1. Oxidosqualene – Lanosterol Cyclase

2.1.1. Substrate Conformation

It is therefore abundantly clear that tight enzymatic control of substrate conformation is a prerequisite for the highly selective formation of products such as lanosterol or hopene. As is evident from Figure 2, the enzyme-imposed substrate conformation is notably different for the formation of lanosterol (**6**) and hopene (**3**). While squalene – hopene cyclase allows an all chair conformation of squalene, oxidosqualene – lanosterol cyclase enforces a chair – boat – chair conformation of its substrate, as demonstrated by the configuration of trapped intermediates described below.

Experiments with the 20-thia analogue **9** of oxidosqualene (Figure 3) and the lanosterol synthase of *Saccharomyces cerevisiae* demonstrated that this compound was neither a substrate nor an efficient inhibitor of the enzyme,[13] in dramatic contrast to 20-oxaoxidosqualene (**10**)[13, 14] which undergoes cyclization to two tetracyclic products (see below). It has been argued that the larger size of sulfur relative to CH_2 or O may result in a somewhat different conformation of **9**, poorer binding to the cyclase, and an enzyme – substrate complex in which the enzymatic acid is not correctly positioned to activate the oxirane function. The reported lack of action of rat liver lanosterol synthase on 11-fluorooxidosqualene (**11**)[15] may be caused by a similar effect, since the steric or electronic differences in this analogue may disfavor the chair – boat – chair folding arrangement, possibly due to steric repulsion between the fluorine at C11 and the methyl group at C6, as is evident in Figure 2. Implicit in this argument is the assumption that the conformer of oxidosqualene which binds to and complements the enzyme


G. E. Schulz


D. R. Liu


K. U. Wendt


E. J. Corey

Georg E. Schulz, was born in 1939 in Berlin, studied physics at the Technical University of Berlin and the University of Heidelberg, and obtained his PhD. in 1966 working with O. Haxel. After postdoctoral studies with H. Wychoff und F. Richards at Yale University, he moved in 1969 to the group of K. Holmes at the Max-Planck Institute for medicinal research in Heidelberg. There, he founded a group for protein crystallography. Since 1984 he has been Professor for Biochemistry at the University of Freiburg, where he runs a protein structure function school for chemistry students.

David R. Liu was born in Riverside, California in 1973. He received his B.A. in chemistry from Harvard University in 1994, where he conducted research on steroid biosynthesis under the guidance of E. J. Corey. David performed his doctoral research in P. G. Schultz's group at the University of California, Berkeley, investigating in vitro and in vivo methods for the site-specific incorporation of unnatural amino acids into proteins. In 1999, David assumed the position of Assistant Professor of Chemistry and Chemical Biology at Harvard University, where his research efforts are focused on the chemistry and biology of molecular evolution.

Karl Ulrich Wendt was born in 1968 in Essen, Germany. He received his Diploma (1994) and Ph.D. (1998) from the University of Freiburg, Germany, where he worked under the direction of G. E. Schulz on the expression, purification, and X-ray structural analysis of squalene – hopene cyclase. In 1998 he joined the groups of P. G. Schultz and R. C. Stevens at the University of California, Berkeley, working on the the structural consequences of antibody maturation. He has done further postdoctoral work in the protein crystallography group in the Department of Protein Engineering at Genentech, Inc. in South San Francisco, USA.

Elias J. Corey, born in 1928 in Methuen, 30 miles north of Boston, studied chemistry from 1945 – 1950 at the Massachusetts Institute of Technology, where he gained his doctorate for work on synthetic penicillins under the supervision of J. C. Sheehan. In January 1951 he joined the University of Illinois at Urbana-Champaign as an Instructor in Chemistry and was promoted in 1956 to full Professor. Since 1959 he has been at Harvard University. For as long as he can remember he has enjoyed study, adventure, and discovery.

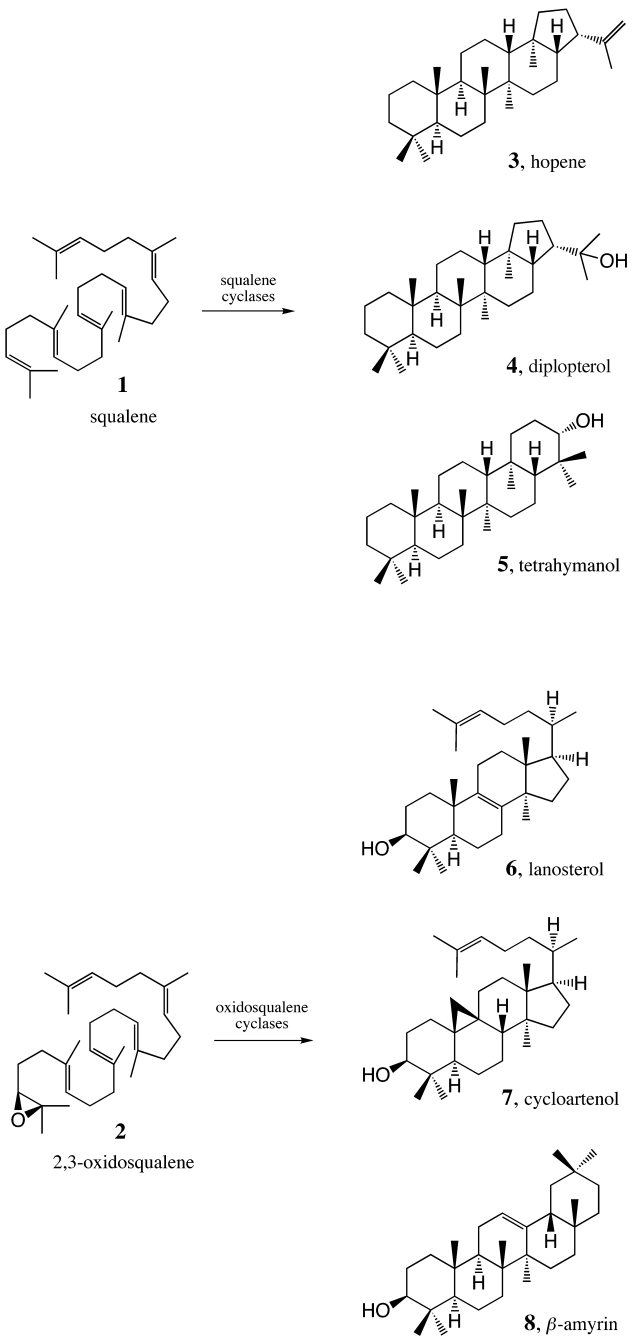

Figure 1. Substrates and products of several triterpene cyclase enzymes.

pocket has a molecular geometry which allows cyclization to proceed with a minimum of conformational change in the substrate once the reaction is initiated. This notion is attractive from a chemical point of view because it restricts the modes of reaction which are available to any intermediate carbocations and leads to the most efficient channeling of the cyclization to one product.

Consistent with the above possibilities, it has been reported that neither 14-fluorooxidosqualene (**12**) nor 14,15-dihydrooxidosqualene (**13**) afford any cyclic products when incubated with rat liver oxidosqualene cyclase (Figure 3).[16] The 14-fluoro substituent may interact repulsively with either the methyl group at C10 or a nearest neighbor from the

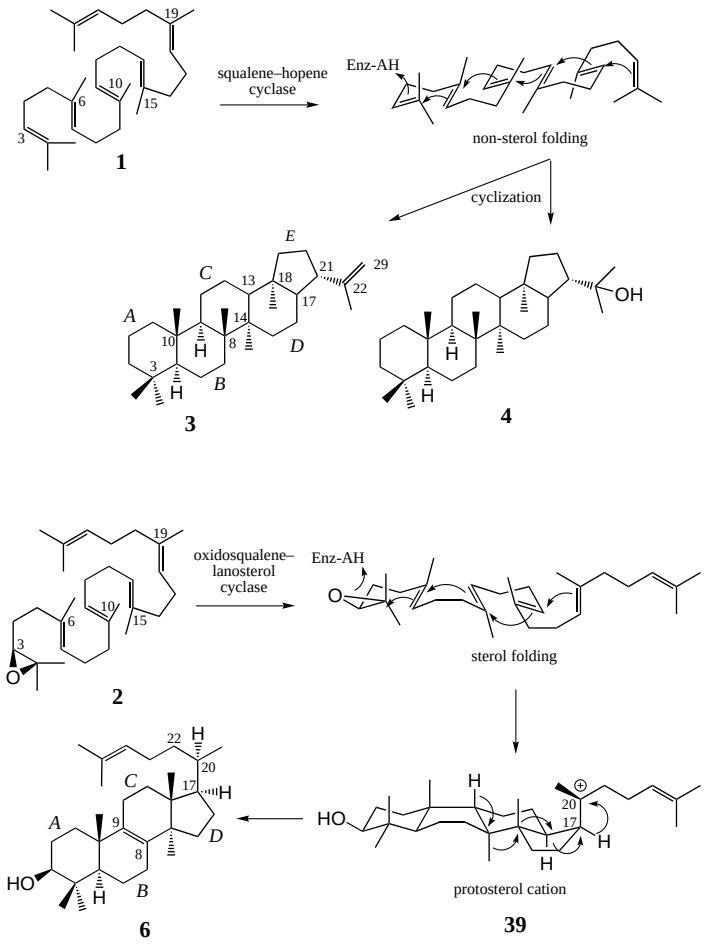

Figure 2. Putative substrate conformation and overall mechanism for reactions catalyzed by oxidosqualene–lanosterol cyclase and squalene–hopene cyclase.

enzyme binding pocket which would lead to incorrect folding of substrate and loss of epoxide activation.

2.1.2. Epoxide Opening and A-Ring Formation

The chemical cyclization of oxidosqualene must be initiated by electrophilic epoxide activation. Oxidosqualene is completely stable in neutral media and is even quite stable in glacial acetic acid at room temperature for up to one day. A more powerful Brønsted acid such as trichloroacetic acid is required for sufficiently strong epoxide activation to promote cyclization on a shorter timescale.[10] As a single aspartic acid residue (D456) in the oxidosqualene cyclase (lanosterol synthase) of *S. cerevisiae* was found to be critical for cyclization[17, 18] and Lewis acidic metals are absent in the purified active enzyme,[17] a kinetic and mechanistic study of proton catalysis of cyclization was undertaken with simpler models of oxidosqualene **14**–**16** (Figure 4).[10]

The rates of proton-catalyzed carbocyclization of substrates **14** and **15** were considerably greater than the rate of proton-catalyzed carbocation formation from the noncyclizable substrate **16**, consistent with concerted C–O cleavage and cyclohexane C–C bond formation for **14** and **15**.[10] As expected, anchimeric assistance to C–O cleavage by the

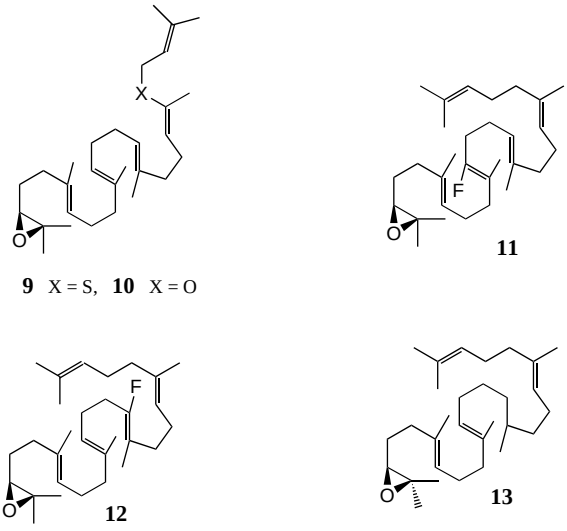

Figure 3. Substrate analogues of oxidosqualene-lanosterol cyclases which provide insight into substrate conformation.[13–16]

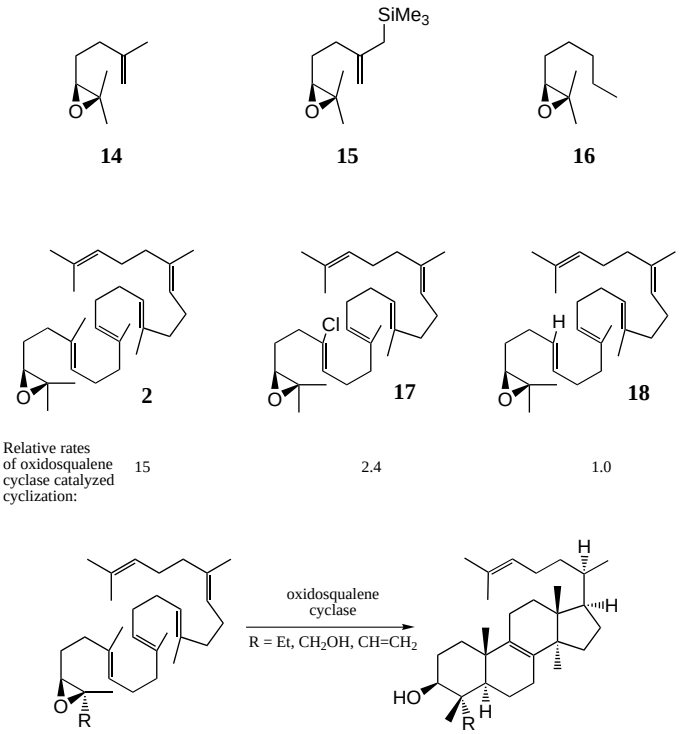

Figure 4. Evidence for concerted epoxide opening and A-ring closure catalyzed by oxidosqualene – lanosterol cyclases.[17]

proximate double bond was greater for the more nucleophilic olefin **15** than for the less π-nucleophilic **14**.[10] Since the conformers of **14** and **15** which correspond to the optimal geometry for cation – π-olefin cyclization constitute only a minor fraction of the rotamers of **14** and **15** which are present in solution, there would presumably be even greater anchimeric acceleration for the cyclization of the optimally prefolded conformers. Thus, the combination of optimal placement of the activating proton source relative to the epoxide oxygen and the optimal folding of the substrate could together produce rapid catalytic cyclization, which would explain how an enzyme-provided carboxylic acid could initiate cyclization of oxidosqualene. Even greater accelerations would be expected on chemical and mechanistic grounds if the enzyme provides one or two hydrogen-bond donors to the key catalytic carboxylic acid.

Early qualitative studies of Lewis acid initiated cyclizations of oxidosqualene analogues suggested that during $SnCl_4$-catalyzed reaction in benzene, epoxide cleavage and cyclohexane ring formation are concerted.[19] Recent kinetic studies of the *S. cerevisiae* lanosterol synthase demonstrate that this enzyme catalyzes the cyclization of epoxides **2**, **17**, and **18** with the relative rates shown in Figure 4. The correlation between the observed rates of cyclization and π-nucleophilicity of the C6,C7 double bond of substrates **2**, **17**, and **18** provides additional evidence for concerted C–O cleavage and A-ring formation for the enzymatic cyclization.[17] The configuration of products resulting from the enzymatic cyclization of oxidosqualene analogues bearing modified α-C2 methyl groups (Figure 4)[20–23] demonstrates that A-ring closure occurs faster than rotation about the C2–C3 bond. This observation is also consistent with, although not exclusively indicative of, a concerted mechanism. Finally, recent computational results are also in agreement with these experimental findings suggesting concerted epoxide opening and A-ring formation.[12, 24]

2.1.3. B- and C-ring cyclization

Formation of the B ring as a boat conformer probably occurs very rapidly once positive charge builds on C5 of the A ring. It is not known, however, if there is any temporal overlap between the formation of the A and B rings. The closure of the third ring has also long been enigmatic because direct formation of a six-membered C ring would represent an anti-Markovnikov mode of addition to a double bond. Closure of a six-membered ring would, however, be stereoelectronically somewhat more favorable than Markovnikov cyclization to form a five-membered C-ring. A key piece of information relevant to this dilemma was obtained from the products arising from the cyclization of 20-oxaoxidosqualene (**10**) by the lanosterol synthase of *S. cerevisiae*. In addition to the expected 6-6-6-5 fused ring product **19** (40%), incubation of **10** also affords the 6-6-5 fused ring product **20** (3.4%).[13] The formation of **20** is most easily explained by internal trapping of the carbocation **21** through intramolecular reaction with the electron-rich C18,C19 double bond (Figure 5).

Additional substrate analogue incubations provide further evidence for a five-membered C-ring closure followed by a ring expansion (Figure 6). Oxidosqualene cyclase processes 15-ethyloxidosqualene (**22**) into a 71:29 mixture of ethyl lanosterol and a 6-6-5 tricyclic product,[25] converts 18,19-dihydrooxidosqualene (**23**) into a 6-6-5 tricyclic product,[26] transforms the 20-carbon truncated analogue **24** of oxidosqualene into three 6-6-5 tricycles,[27] and cyclizes 10,15-didemethyloxidosqualene (**25**) into predominantly a 6-6-5-4 system in the product **26** (Figure 6).[28] The structural diversity of these substrate analogues makes it unlikely that they all cyclize following a pathway that is not relevant to that of the natural substrate. It should be noted that the substrate

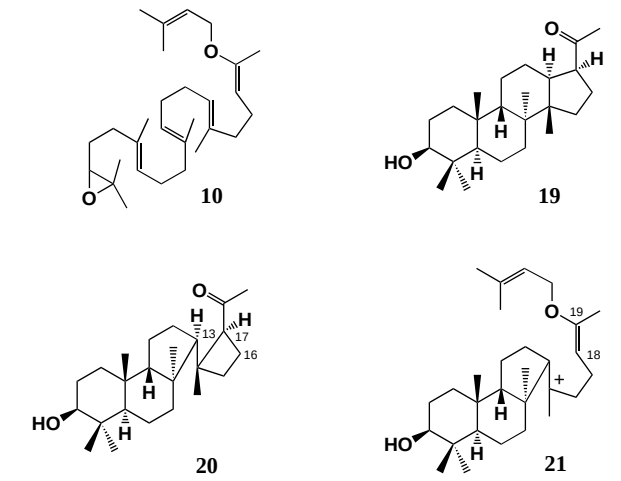

Figure 5. Substrate analogues and products of oxidosqualene cyclase which are suggestive of a five-membered C-ring intermediate.[13]

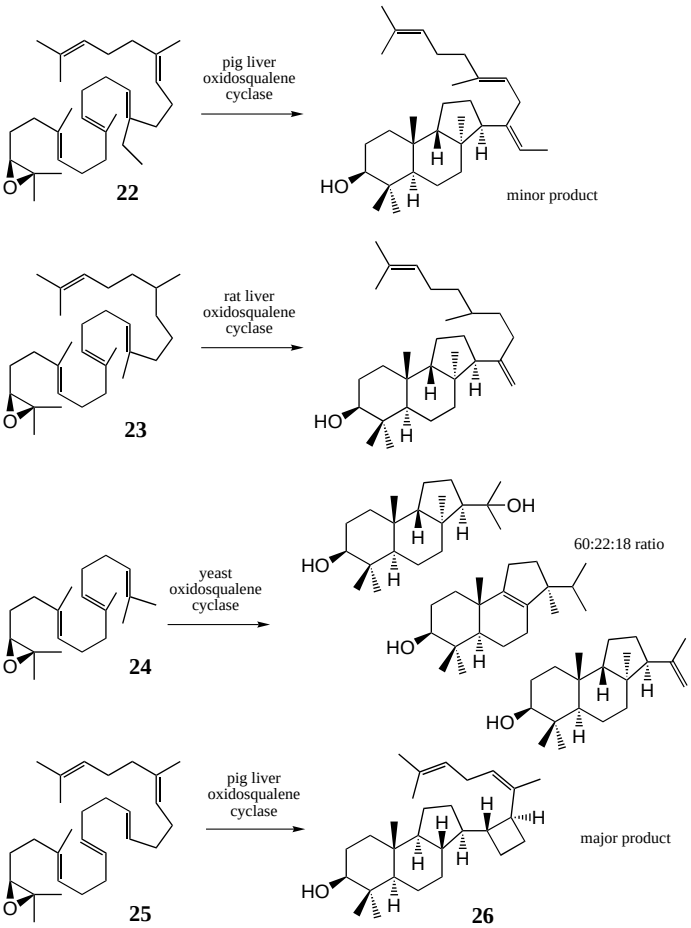

Figure 6. 6-6-5 cyclization products formed by oxidosqualene cyclases.[25–28]

conformation which is required to explain the stereochemistry of the conversion **25** → **26** is the nonsteroidal B-chair type, implying that the cyclase not only recognizes the difference between methyl and hydride substituents at C10, but also that this structural feature is critical to the proper double bond face selectivity in the closure of the B ring. This finding also argues that the fit between the substrate and the enzyme pocket is remarkably precise in some areas. Collectively these results suggest that substrate perturbations around C10, C15, and C19 of oxidosqualene reduce the enzyme's ability to effect ring expansion relative to further cyclization of the C15 carbocation. Computational evidence provides further support for the 6-6-5 to 6-6-6 rearrangement pathway.[12]

2.1.4. Protosterol Cation Formation and Rearrangement to Lanosterol

Early analyses of the stereochemistry of sterol biosynthesis assumed that the enzymatic conversion of oxidosqualene to lanosterol proceeds via a protosterol cation in which the cationic side chain at C17 is α-oriented (steroid notation) as shown in compound **27** (Figure 7).[3] A problem with the

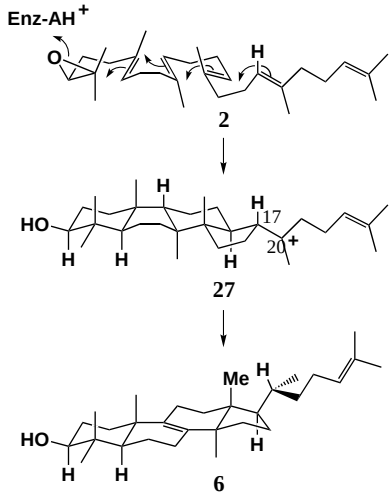

Figure 7. The formerly postulated, incorrect C17 stereochemistry of protosterol requires a large side-chain rotation prior to rearrangement to account for the observed stereochemistry at C20.[31]

intermediacy of **27** is that it would be expected to lead, after hydride migration from C17 to C20, not to the natural sterol 20*R* configuration, but to the unnatural 20*S* arrangement. Starting from the geometry of **27** produced immediately after D ring closure, a rotation about the C17–C20 bond of 120° is required prior to hydride migration in order to produce the natural 20*R* configuration of lanosterol (**6**), whereas only a 60° rotation is required to produce the unnatural 20*S* configuration (Figure 7). Perhaps because of this difficulty, it was proposed that the initial tetracyclic intermediate may not be cation **27** but a covalent adduct formed by reaction of **27** with a nucleophilic group of the cyclase.[29, 30] Isolation of a trapped protosterol (methyl ketone **19**) from the enzyme-catalyzed cyclization of 20-oxaoxidosqualene (**10**), however, demonstrated the β (pseudoaxial side chain) rather than α (pseudoequatorial side chain) stereochemistry at C17 of protosterol (Figure 8).[31] This finding removed the need to invoke either large (120°) rotation around the C17–C20 bond prior to rearrangement, or covalent attachment of a transient enzyme nucleophile. Interestingly, protosterol analogue **28** is only a weak inhibitor of yeast oxidosqualene cyclase (with an IC_{50} which is 55-fold higher than that of 2,3-iminosqualene (**29**)),

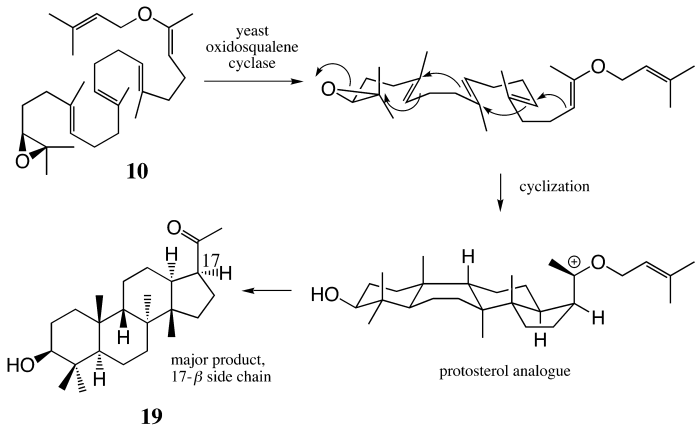

Figure 8. Trapping of an enzyme-cyclized protosterol analogue.[31]

suggesting that the protosterol cation is not bound very snugly by the enzyme (Figure 9).[32] The 17β orientation of the side chain in the protosterol cation was also demonstrated by the action of the yeast cyclase on 20,21-dehydrooxidosqualene (**30**). Enzymatic cyclization of **30** yielded protosterol derivative **31** (Figure 10), which was identical with a totally synthetic sample.[14]

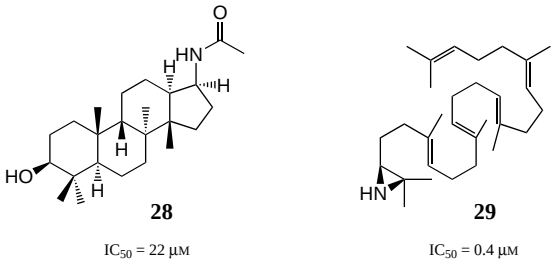

Figure 9. A comparison of oxidosqualene cyclase inhibitors suggests that the protosterol cation is weakly bound by the enzyme.[32]

The isolation of this trapped protosterol analogue enabled the first examination of the rearrangement process uncoupled from the cyclization events. Nonenzymatic reaction of the benzoate of **32** (that is, **33**) with BF_3 in dichloromethane at $-90\,^{\circ}C$ for 3 min produced 24,25-dihydroparkeol benzoate (**34**) via the protosterol cation **35** (Figure 10).[31] Similarly, the BF_3-induced rearrangement of the C20 diastereomer of **33** produced mainly the C20 diastereomer of **34**.[14] The BF_3-catalyzed rearrangements of the 17α epimer of **33**, and its C20 epimer, in contrast, are nonselective at C20, each giving a 1:1 mixture of C20 epimers of dihydroparkeol benzoate (**36**).[33] Consistent with these nonenzymatic findings, the enzymatic incubation of substrate analogues bearing significant structural differences from oxidosqualene still leads to some hydride and methyl group rearrangement. The cyclase-catalyzed cyclization of a precyclized (D ring) analogue of oxidosqualene (**38**) yields rearranged lanosterol-like products (Figure 11),[34, 35] while the enzymatic cyclization of a truncated substrate analogue (**24**) which yields unnatural 6-6-5 tricycles is also accompanied by methyl group migration (Figure 6).[27] Importantly, even the nonenzymatic Lewis acid catalyzed cyclization of oxidosqualene affords at least one

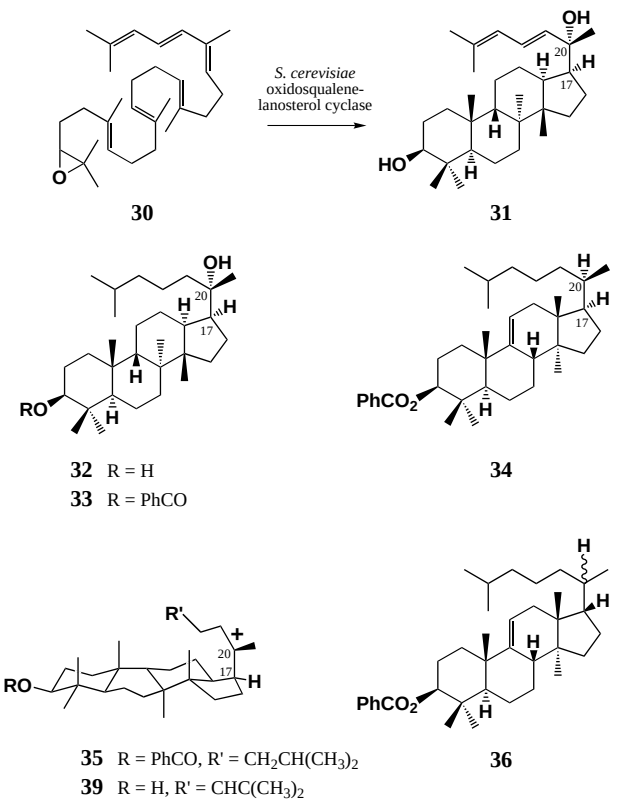

Figure 10. Products which are suggestive of the stereochemical pathway of nonenzymatic rearrangement.[33]

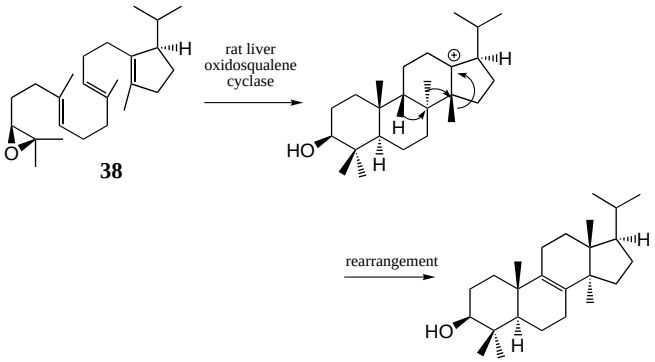

Figure 11. Enzymatic cyclization and rearrangement of a precyclized oxidosqualene analogue.[34]

product arising from methyl group migration, further suggesting the ease with which these rearrangement processes naturally occur (Figure 12).[36]

These results provide several crucial insights into the molecular details of the cyclization and rearrangement steps of lanosterol biosynthesis. First, the protosterol cation **39** (Figures 2 and 10) undergoes C17−C20 hydride migration to form the 20*R* product at a rate which is rapid relative to rotation about the C17−C20 bond. Second, this bond rotation is greatly retarded in the 17β protosterol side-chain arrangement, probably because of repulsion with the nearby 14β-methyl group of **39**. Third, the pathway involving a 17β side chain for the protosterol cation, as in **39**, allows for much more rigorous control by the enzyme of the C20 configuration in lanosterol than would the hypothetical pathway with the 17α

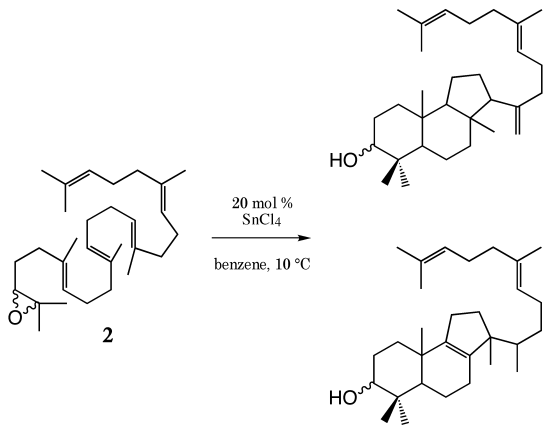

Figure 12. Nonenzymatic cyclization of oxidosqualene.[36]

orientation of the side chain, corresponding to **27** of Figure 7. Finally, it is clear that the rearrangements of hydride and methyl substituents which convert the protosterol cation into lanosterol can proceed spontaneously without intervention by lanosterol synthase, except for the final proton removal step. This deprotonation clearly must be under rigorous control by the enzyme. The enzyme's primary role during the rearrangement of protosterol, therefore, may simply be to protect the intermediate cations from quenching by water (by exclusion of water from the active site) and from elimination (by exclusion of bases from the active site) prior to deprotonation by a well-positioned enzymatic base.

2.2. Squalene – Hopene Cyclase

2.2.1. Initiation and Early Cyclization Events

The bacterial squalene cyclases catalyze a stereochemically and mechanistically simpler process than the eukaryotic oxidosqualene cyclases. These squalene cyclases do not employ the same substrate conformation as lanosterol synthase but instead allow the substrate to adopt an all chair-like geometry (Figure 2). Furthermore, skeletal rearrangement following cyclization is not generally observed in the unperturbed catalytic pathways of these enzymes, unlike their oxidosqualene cyclase counterparts. The lower basicity of a carbon – carbon double bond relative to the epoxide group suggests that the squalene cyclases provide a catalytic acid at least as strong as that used to initiate the cyclization of oxidosqualene. Consistent with this hypothesis, the bacterial squalene cyclases accept oxidosqualene and many of its analogues as substrates for cyclization.[9] While no chemical studies on squalene cyclases have elucidated the mechanism of A- and B-ring formation, it is tempting to assume, in analogy with the oxidosqualene cyclases, that A-ring closure is concerted with olefin protonation since anchimeric assistance may significantly accelerate protonation of the relatively nonbasic 2,3-olefin.

In contrast with the oxidosqualene cyclases, substrate analogue studies suggesting a five-membered C-ring intermediate followed by ring expansion during the cyclization of squalene by squalene – hopene cyclase have only emerged very recently. Squalene – hopene cyclase from *Alicyclobacillus acidocaldarius* processes a truncated alcohol **40** into a 6-6-5 product consistent with trapping of a Markovnikov cation generated from five-membered C-ring closure (Figure 13).[37]

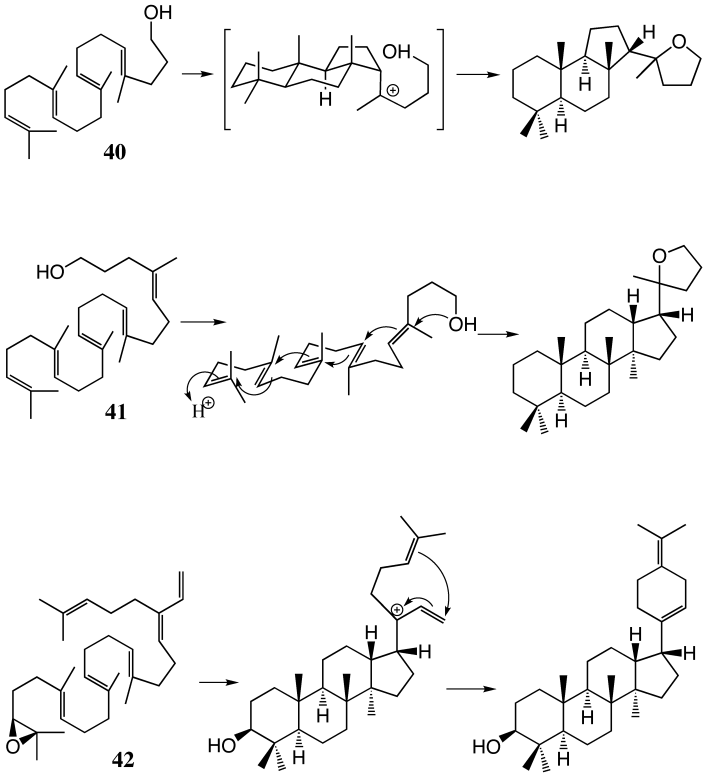

Figure 13. Evidence for five-membered D-ring formation during squalene cyclization.[38, 39] In each case, squalene – hopene cyclase from *A. acidocaldarius* was used.

No 6-6-6 products corresponding to trapping of an anti-Markovnikov cation arising from six-membered C-ring formation were detected. The prospects of a Markovnikov versus anti-Markovnikov mechanism for C-ring closure are discussed further in light of recent structural biology and site-directed mutagenesis studies (see below).

2.2.2. D-Ring Formation

Chemical studies strongly suggest that D-ring cyclization catalyzed by squalene cyclases proceeds through a five-membered ring closure to afford a Markovnikov cation followed by ring expansion to yield a 6-6-6-6 system in a mechanism similar to C-ring closure catalyzed by the oxidosqualene – lanosterol cyclases. Incubation of a truncated squalene analogue **41** with squalene – hopene cyclase leads to almost quantitative formation of a 6-6-6-5 product which may arise from trapping of an intermediate C18 Markovnikov carbocation (Figure 13).[38] Similarly, incubation of 29-methylidene-oxidosqualene (**42**) with squalene – hopene cyclase provides a 6-6-6-5 product (Figure 13) and concomitant irreversible inactivation of the cyclase (see below).[39] Cycli-

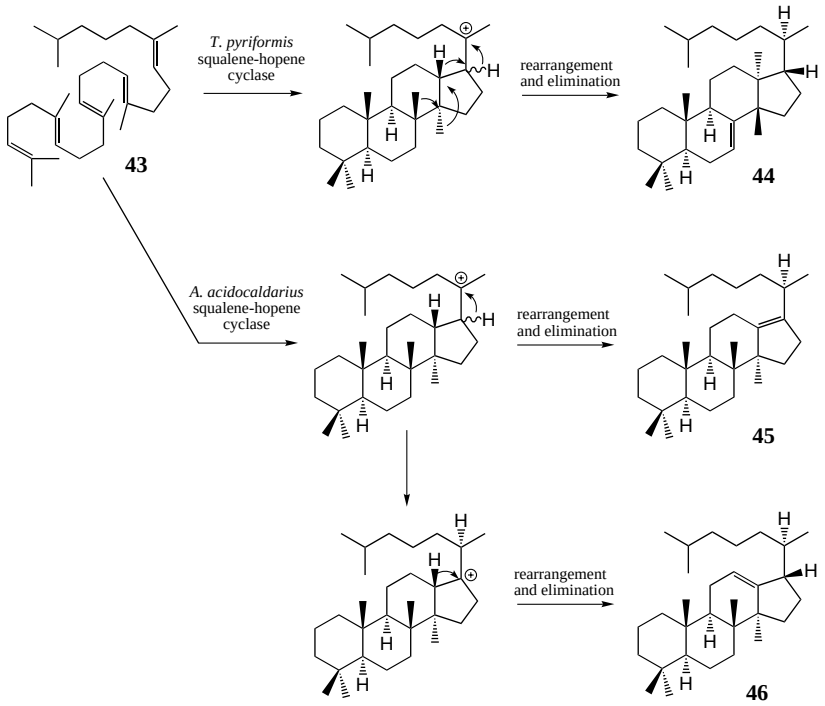

Figure 14. Additional evidence for five-membered D-ring formation during squalene cyclization.[40, 41]

zation of 2,3-dihydrosqualene (**43**) also leads to trapping of a 6-6-6-5 intermediate yielding three products (**44**–**46**) from two different squalene cyclases (Figure 14).[40, 41] Importantly, 6-6-6-5 compounds (**47**–**51**) have also been observed as minor products in the natural turnover of squalene with squalene–hopene cyclase from *A. acidocaldarius* (Figure 15).[42] This finding represents the first evidence for five-membered D-ring closure that is free from any bias which could be introduced by stereochemical perturbations arising from substrate analogues or enzyme active-site mutants.

2.2.3. E-Ring Formation, Rearrangement, and Elimination

The importance of generating a Markovnikov carbocation during enzyme-catalyzed five-membered E-ring closure is exemplified by the finding that squalene analogues **52** and **53**, which lack one terminal methyl group and therefore cannot form a tertiary carbocation upon E-ring cyclization, yield tetrahymanol-like 6-6-6-6-6 products **54** and **55** upon incubation with squalene–hopene cyclase (Figure 16).[43] The structural elucidation of tetracyclic compounds **44**–**46** arising from incubation of 2,3-dihydrosqualene (**43**) with *Tetrahymena pyriformis* and *A. acidocaldarius* squalene cyclases indicate the occurrence of hydride and methyl group rearrangements in these products (Figure 14).[9] Moreover, the collection of side products arising from the action of *A. acidocaldarius* squalene–hopene cyclase on its natural substrate also includes a number of partially rearranged tetracycles **49**–**51** (Figure 15).[42] These findings are consistent with the oxidosqualene cyclase model described above, in which skeletal rearrangement occurs spontaneously in the absence of base or water to quench carbocations. The partitioning between hopene (**3**; 80%) and the water-quenched diplopterol (**4**; 20%) during the natural action of squalene–hopene cyclases suggests significant water accessibility to the termination region of the active site.[44]

3. The Reaction Pathway: Biological Studies

Molecular and structural biologists have joined chemists in probing the mechanism of enzyme-catalyzed triterpene formation. The last seven years have witnessed the cloning and sequence elucidation of at least 15 putative triterpene cyclases: Those from *Homo sapiens*,[45] *Rattus norvegicus*,[46, 47] *Candida albicans*,[48, 49] *Saccharomyces cerevisiae*,[50, 51] *Schizosaccharomyces pombe*,[52] *Arabidopsis thaliana*,[53] *Panax ginseng*,[54] *Alicyclobacillus acidocaldarius*,[55] *Zymomonas mobilis*,[56] *Bradyrhizobium japonicum*,[57] *Methylococcus capsulatus*,[58] *Rhodopseudomonas palustris*,[58] *Rhizobium*,[59] *Synechocystis*,[60] and *Bacillus subtilis*.[61] In 1997 the first three-dimensional structure of a triterpene cyclase (squalene–hopene cyclase from *A. acidocaldarius*) was solved.[62–64] This structure, together with additional biological studies, has produced a wealth of mechanistic insight into both squalene and oxidosqualene cyclases.

3.1. The Squalene–Hopene Cyclase Structure

Squalene–hopene cyclase is a homodimeric enzyme with 631 amino acids (71.5 kD) per subunit.[55, 63, 65] The peptide chain of each subunit is organized in two mainly α-helical domains, which together form a dumbbell-shaped molecule of 50 Å diameter and 70 Å height (Figure 17). Domain 1 is a regular $(\alpha/\alpha)_6$ barrel, while domain 2 assumes a similar but less regular α-barrel fold. The structural alignment of both domains indicates that domain 2 may be derived from domain 1 by an early gene duplication.[66] The two domains are connected by long loops which together enclose a large central cavity of 1200 Å^3 (Figure 17). A second cavity of 400 Å^3 (the "upper cavity") is located in the center of the $(\alpha/\alpha)_6$ barrel in domain 1.[64]

The structure suggests that the active site is localized in the enzyme's central cavity, where the competitive inhibitor *N*,*N*-dimethyldodecylamine-*N*-oxide (LDAO)[67] is bound (Figure 18).[63] This view is confirmed by an abundance of biochemical and structural evidence. Residues Asp376 and Asp377, which contact the upper part of the central cavity, have been shown by site-directed mutagenesis to be essential for catalysis in squalene–hopene cyclase.[68] Mutations at nearby residues Asp374 and His451 also lower the catalytic efficiency of the enzyme.[69] Asp456 of *S. cerevisiae* oxidosqualene–lanosterol cyclase corresponds to Asp376 by se-

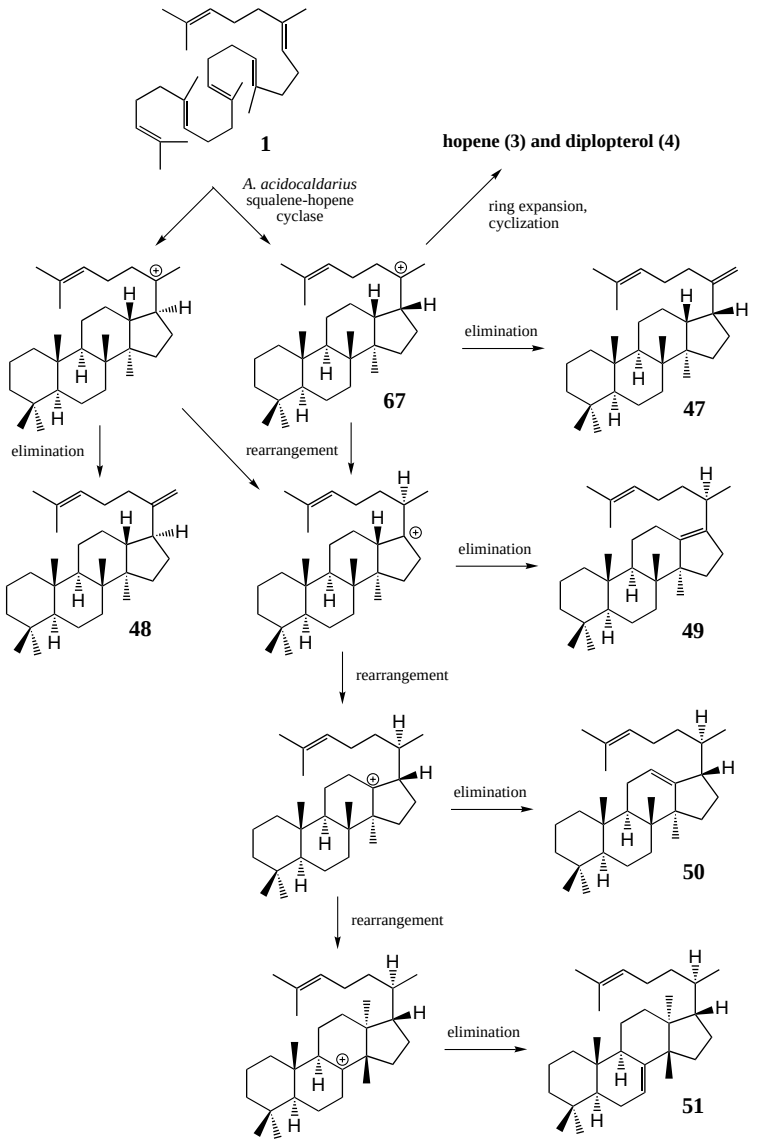

Figure 15. Formation of minor side products in the natural reaction catalyzed by squalene–hopene cyclase.[42]

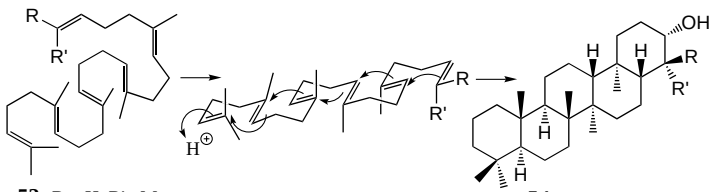

52: R = H, R'= Me
53: R = Me, R' = H
54: R = H, R'= Me
55: R = Me, R' = H

Figure 16. Substrate analogues that yield tetrahymanol-like 6-6-6-6-6 products upon cyclization with squalene–hopene cyclase.

quence alignment and is also required for enzyme activity.[18] Additional evidence for placing the active site of squalene–hopene cyclase within the central cavity emerges from the mutagenesis of residues lining this cavity, which results in the formation of altered products.[38, 69–73] Furthermore, several mechanism-based inhibitors of oxidosqualene–lanosterol cyclases covalently label amino acids corresponding to central-cavity residues of squalene–hopene cyclase.[18, 74] Finally, the topological position of the active site with respect to the (α/α)-barrel folds is equivalent to the position of active sites commonly found in other (α/α)-barrel proteins.[63]

Squalene and oxidosqualene cyclases share a unique sequence repeat (referred to as a "QW repeat") with the consensus sequence: a-b-$x_{2\text{-}3}$-c-d-x_3-Gln-$x_{2\text{-}5}$-Gly-x-Trp, where a = Lys or Arg, b = Gly or Ala, c = Phe, Tyr, or Trp, and x = any residue.[75] This repeat typically occurs five times in oxidosqualene cyclases and up to eight times in the squalene cyclases. The high conservation of this repeat throughout the triterpene cyclases has led to hypothesis that the conserved Trp may be involved in the stabilization of intermediate carbocations,[76] consistent with earlier active-site models which proposed a structurally defined[9] arrangement of aromatic amino acids to stabilize carbocationic intermediates.[50, 77, 78] Such an arrangement has also been suggested to induce the different transition state conformations in squalene versus oxidosqualene cyclases.[79] The structure of squalene–hopene cyclase, however, demonstrates that these QW-repeats are not located in the active-site cavity but rather at the surface of the enzyme (Figure 17) where the conserved amino acid residues of the repeats form an intricate network of hydrogen-bonding and hydrophobic interactions that connect the α helices of the $(\alpha/\alpha)_6$ barrel of domain 1.[63, 64] It has been proposed that this arrangement might stabilize the triterpene cyclases against the reaction enthalpy released during cyclization.[63]

3.2. Membrane Binding

Cellular localization and solubilization characteristics suggest that the triterpene cyclases are integral membrane proteins.[44, 80] The three-dimensional structure of squalene–hopene cyclase identifies the enzyme as a monotopic membrane protein[81] that interacts with the nonpolar portion of the phospholipid bilayer without protruding through the membrane (Figure 19).[64] The membrane-binding region forms a flat nonpolar surface of 1600 Å^2, the center of which is an opening to an extended channel connecting the active-site cavity with the interior of the phospholipid bilayer. [63, 64] This arrangement most likely provides a path for the exchange of squalene (**1**) and the products hopene (**3**) and diplopterol (**4**) between this cavity and the nonpolar section of the lipid bilayer where these nonpolar compounds are expected to reside.

The large size and rigidity of the cyclization products together with the hydrophobicity of the active site raise the interesting possibility that triterpene cyclases may undergo relative domain motions during product release. No indication for this, however, has yet been observed in the squalene–hopene cyclase crystal structures. An analysis of

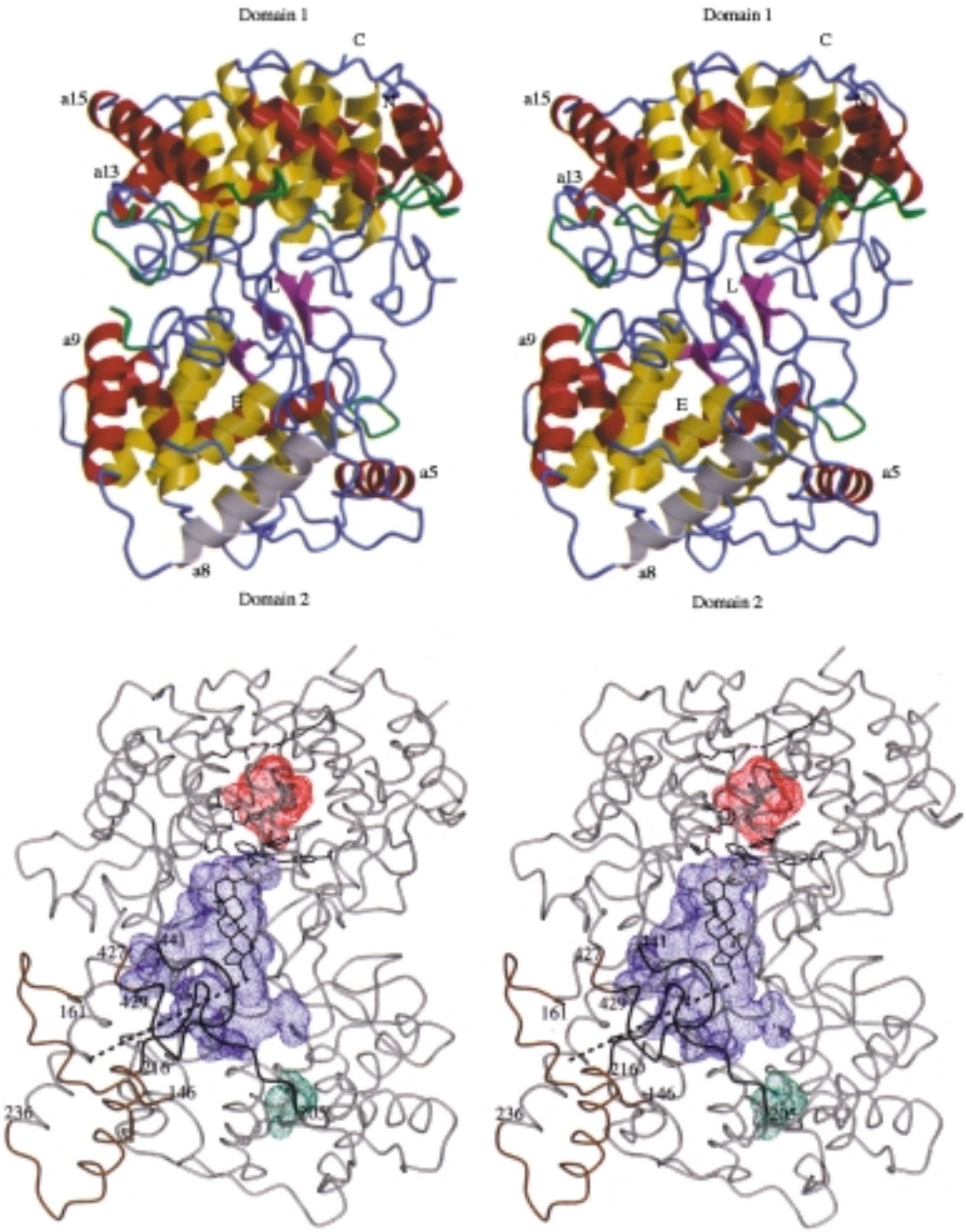

Figure 17. Overall structure of *A. acidocaldarius* squalene–hopene cyclase. Upper stereo view: Ribbon representation of one subunit of the dimeric enzyme with labels at the termini of the peptide chain (N and C), the position of the competitive inhibitor LDAO (L), and the entrance of the active-site channel (E). Color coding: inner and outer helices of the (α/α) barrels are yellow and red, respectively, the β structure is purple, the QW motifs are green, and helix α-8 in the suggested membrane-binding region is white. Lower stereo view: Cα chain trace of the cyclase. The three main cavities[103] within the structure are colored: The active-site cavity is blue, the upper water-filled cavity is red, and a smaller water-filled cavity in domain 2 is green. Highlighted are the membrane-binding region (yellow; residues 146–161, 216–236, and 427–429) and mobile loops (dark; residues 205–216 and 429–441) that presumably open for the substrate entrance through a channel (dashed line) that connects the membrane binding region with the active site. The picture contains a modeled molecule of the product hopene (see text).

crystallographic B-factors in the enzyme structure suggests that the gating loops of the entrance channel are mobile enough to permit the passage of the bulky and rigid nonpolar products to and from the nonpolar section of the membrane.[63, 64] In the absence of additional structural data, it remains to be determined if or how the enzyme avoids energetically unfavorable scenarios between turnovers, such as the uptake of water into the nonpolar 1200 Å^3 central cavity.

The membrane-binding regions are oriented approximately in parallel within the dimer of squalene–hopene cyclase (Figure 19a). Such an arrangement is also observed in dimeric prostaglandin-H(2) synthases I and II, which are the only other structurally characterized monotopic membrane proteins (Figure 19c).[82–84] In the squalene–hopene cyclase structure, detergent ligands are bound in a nonpolar pocket at the dimer interface. This pocket may accommodate lipid molecules in vivo and it has been suggested that lipid binding

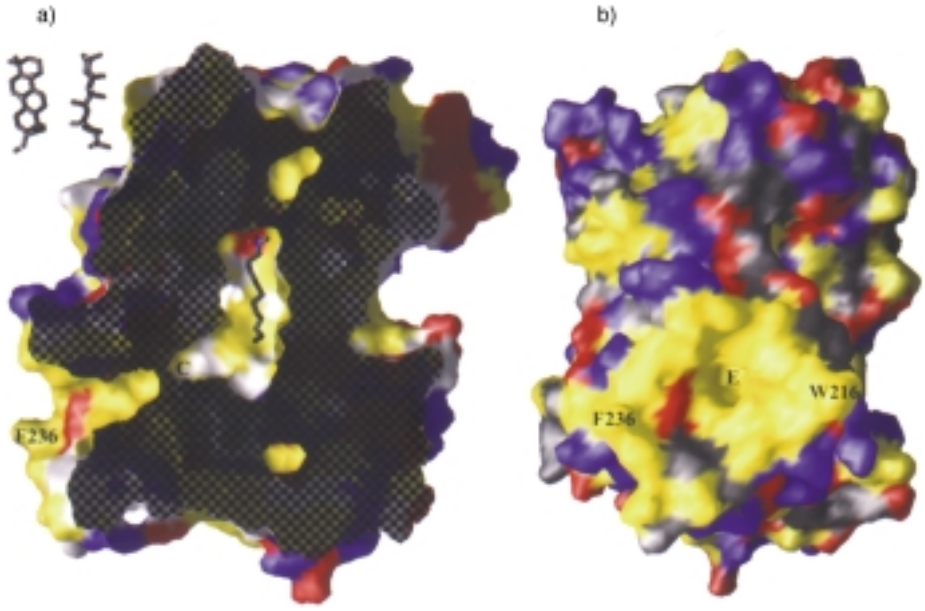

Figure 18. Surface representation[104] of one subunit of *A. acidocaldarius* squalene–hopene cyclase with nonpolar areas (yellow), positively charged areas (blue), and negatively charged areas (red). a) The surface cut (cutting plane checkered) presents a view of the active-site cavity with the bound inhibitor LDAO. The nonpolar entrance channel runs into the extended nonpolar region on the left, which is presumably responsible for integral membrane binding. The channel constriction (C) seems to be closed but is flexible enough to permit substrate passage. In the upper left area, hopane is depicted from two views. b) View of the nonpolar membrane-binding surface centered around the channel entrance (E), rotated by 90° around a vertical axis from (a). A ring of positively charged Arg and Lys residues (blue) around this nonpolar plateau may interact with the membrane's polar phospholipid head groups.

to these pockets may shield the polar dimer interface from water and, thus, link dimer assembly with the insertion of squalene hopene–cyclase into the membrane.[64]

3.3. The Active Site

The active-site cavity of squalene–hopene cyclase consists of an extended central nonpolar section and two smaller polar patches at the top (around Asp376) and bottom (around Glu45) of the cavity (Figure 20).[63] Several of the residues lining this cavity are conserved between squalene and oxidosqualene cyclases (Figure 21). The central section contains a chain of conserved aromatic amino acids that face the cavity and are likely to stabilize cationic intermediates. The top and bottom sections of the cavity are formed by polar hydrogen-bonding networks around Asp376 and Glu45, which were suggested to participate in the initial olefin or epoxide protonation and in the final deprotonation step, respectively.[63]

The assignment of the catalytic acid to one of the polar patches is a prerequisite for further mechanistic discussion. A structure–function examination of these enzymes allows this assignment.[63] The protonation steps catalyzed by squalene and oxidosqualene cyclases occur in the same portion of the substrate, while the deprotonation steps occur in different portions of the product skeleton. Since the mutation of the corresponding residues Asp376 (*A. acidocaldarius* squalene–hopene cyclase) and Asp456 (*S. cerevisiae* oxidosqualene–lanosterol cyclase) in the polar patch at the top of the active-site cavity inactivates these two enzymes,[18, 68] and since the inhibitor LDAO binds with its polar head at this position,[63] it is likely that these residues serve as the proton donor. Consistent with this hypothesis, residues lining the active-site cavity show a gradient in conservation between squalene and oxidosqualene cyclases with high conservation near Asp376 at the top and low conservation near Glu45 at the bottom of the cavity (Figure 21). In view of the similar initiation steps in squalene and oxidosqualene cyclases compared to their diverse termination steps, this evidence supports the role of Asp376 and Asp456 as the catalytic acids that initiate the cyclizations of squalene and oxidosqualene, respectively.[63]

3.4. Mechanism-Based Suicide Inhibitors

The suggested function of Asp376 (*A. acidocaldarius* squalene–hopene cyclase) or Asp456 (*S. cerevisiae* oxidosqualene–lanosterol cyclase) described above is further supported by studies with substrate analogues capable of covalently labeling the enzyme. Tryptic digestion and Edman sequencing of the resulting labeled protein indicate that cations generated at increasing distances from the site of protonation interact with active-site residues at increasing distances from the catalytic aspartate. Incubation of the *S. cerevisiae* enzyme with tritiated 6-demethyloxidosqualene (**56**), 10-demethyloxidosqualene (**57**), or 10,15-didemethyloxidosqualene (**58**) is expected to produce reactive mono- and bicyclic cations. These incubations result in labeling one or more residues between positions 486–512 (Figure 22),[18] among which Tyr510 corresponds to active-site residue Tyr420 of the *A. acidocaldarius* squalene–hopene cyclase (Figure 21). The cyclizations of 20-oxaoxidosqualene (**10**) and of the two truncated dienes **59** and **60** are expected to produce reactive cations in the vicinity of the D ring (Figure 20). These compounds label *S. cerevisiae* oxidosqualene–lanosterol cyclase at His234,[18] which corresponds to Trp169 of squalene–hopene cyclase, a residue more distal to Asp376 than Tyr420 (Figure 21). Similarly, *A. acidocaldarius* squalene–hopene cyclase is labeled with 29-methylideneoxidosqualene (**42**)[39] at a peptide section containing Glu45 located at the bottom of the active site (Figure 20); this is the most likely target for the covalent attack, thereby supporting participation of this residue in the terminal deprotonation step.[85]

In contradiction with these studies and the derived substrate orientation, 29-methylideneoxidosqualene (**42**) labels rat liver oxidosqualene–lanosterol cyclase at Asp456 (*S. cere-*

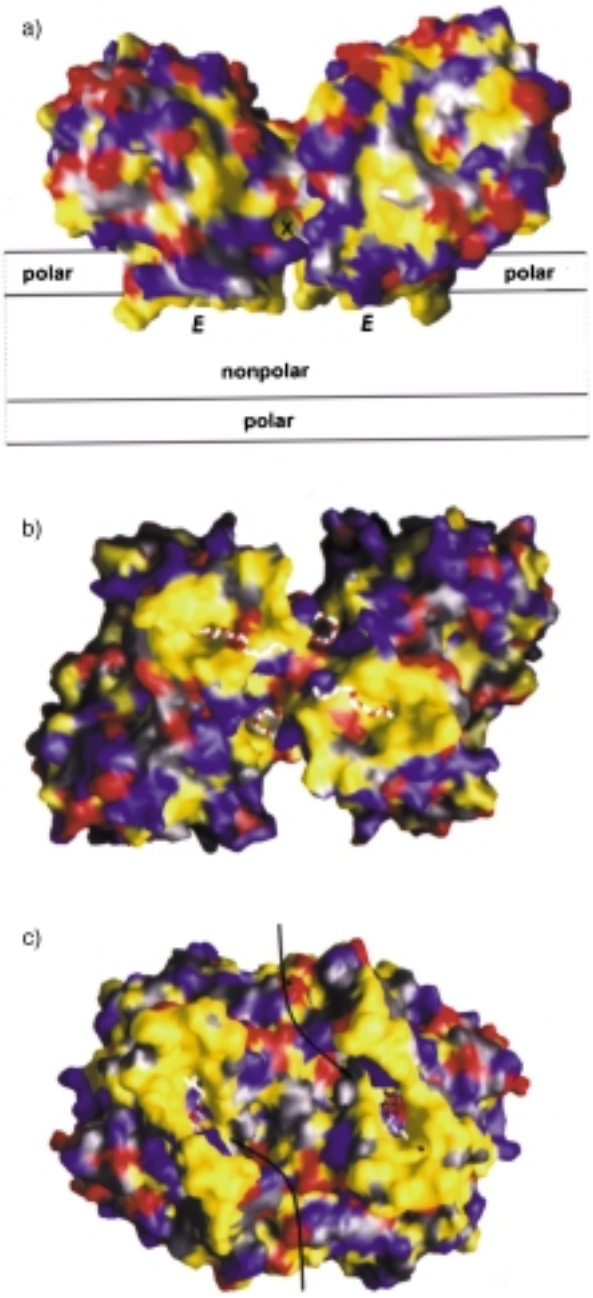

Figure 19. Surface representations[104] of squalene–hopene cyclase from *A. acidocaldarius* (upper two views) and the only other structurally characterized monotopic membrane proteins, prostaglandin-H(2) synthases I and II (lower view).[82–84] The surfaces are color coded with nonpolar regions (yellow), positive regions (blue), and negative region (red). a) Model proposed for the monotopic membrane binding of squalene–hopene cyclase. The nonpolar regions of the protomers are oriented in parallel. This arrangement allows the channel entrances (E) to reach into the nonpolar part of the membrane where squalene is dissolved. A nonpolar pocket, binding a detergent molecule at the dimer interface, is marked (X). b) View from the membrane onto the nonpolar regions of the squalene–hopene cyclase dimer. Several molecules of the crystallization detergent *n*-octyltetraoxyethylene (white) are bound in the high-resolution crystal structure.[64] c) View from the membrane onto the horseshoe-shaped membrane-binding regions of dimeric prostaglandin-H(2) synthase I, with two molecules of the crystallization detergent β-D-octylglucoside bound at the active-site entrance. The arrows indicate a pathway for the polar headgroup of the substrate arachidonic acid toward the active site entrance. Such a passage is not required in squalene–hopene cyclase since its nonpolar substrate does not intercalate between the polar headgroups of the lipid bilayer.

visiae numbering), which suggests that this residue is involved in the stabilization of the protosterol cation (Figure 19).[74] Interestingly, this compound labeled several vertebrate oxidosqualene cyclases but did not label the yeast or plant enzymes.[46] This finding may indicate unusual conformational flexibility or a nonnatural binding orientation of 29-methylideneoxidosqualene in the rat liver enzyme.

3.5. Cation Stabilization

Together with the three-dimensional structure and previously described enzyme-labeling experiments, recent mutagenesis results allow for the first time a detailed discussion of specific π-cation interactions in the triterpene cyclases. Structure-based mutagenesis of conserved residues in the active site of *A. acidocaldarius* squalene–hopene cyclase can alter the partitioning between the main products (hopene and diplopterol) and the side products of unusual structure. Replacement of Asp 377 with Cys or Asn results in the formation of monocyclic compound **61** (Figure 23), suggesting that this residue may stabilize the C10 cation.[37] Similarly, mutation of Tyr 420 to Ala leads to the production of significant amounts of bicyclic triterpenes **62** and **63** and minor amounts of tricyclic compound **64** (Figure 23).[71] The bicyclic compounds may arise from premature quenching of the C10 B-ring cation (C8 in hopene numbering, see Figure 20), which may be stabilized in wild-type squalene–hopene cyclase by its proximity to Tyr 420 (Figure 24). The bicyclic compounds **63** and **65** produced from mutation of Phe 365 to Ala (Figure 23) probably arise by a similar mechanism,[72] which implicates Phe 365 in the stabilization of the bicyclic C8 cation as well (Figures 20 and 24). Replacement of Tyr 609 with Phe similarly resulted in the production of bicyclic triterpene **62**, which suggests that this residue is also involved in the stabilization or positioning of intermediate carbocations.[73] This mutant also produced tetracyclic compounds **47**–**51** at a significantly higher level than the wild-type enzyme.

Mutation of Trp 169 in the center of the active-site cavity (Figure 20) to the less electron-rich residues Phe and His results in increasing amounts of 6-6-6-5 fused ring compound **47** (Figure 15).[38] While wild-type squalene–hopene cyclase produces 0.6 % of **47**, the Trp 169Phe mutant produces 5 % of this compound, while the Trp 169His variant forms 29 % of this compound. Interestingly, mutation of Phe 601 Ala, which is located close to Trp 169 (Figure 20), results in a significant increase in production of **47**, accompanied by lower yields of two 6-6-5 tricyclic compounds **64** and **66** (Figures 15 and 23).[37, 70] These findings suggest that residues Phe 601 and Trp169 may stabilize cation **67** (Figure 15) by π-cation interactions and that Phe601 may interact with a 6-6-5 Markovnikov cation intermediate (Figures 20 and 24). The loss or the perturbation of these interactions may result in the premature quenching of tricyclic and tetracyclic Markovnikov cations to form 6-6-6-5 product **47** and 6-6-5 compounds **64** and **65**.

Surprisingly, mutation of Trp 489, which is adjacent to Tyr 420 in the upper part of the active site (Figure 20), to Phe

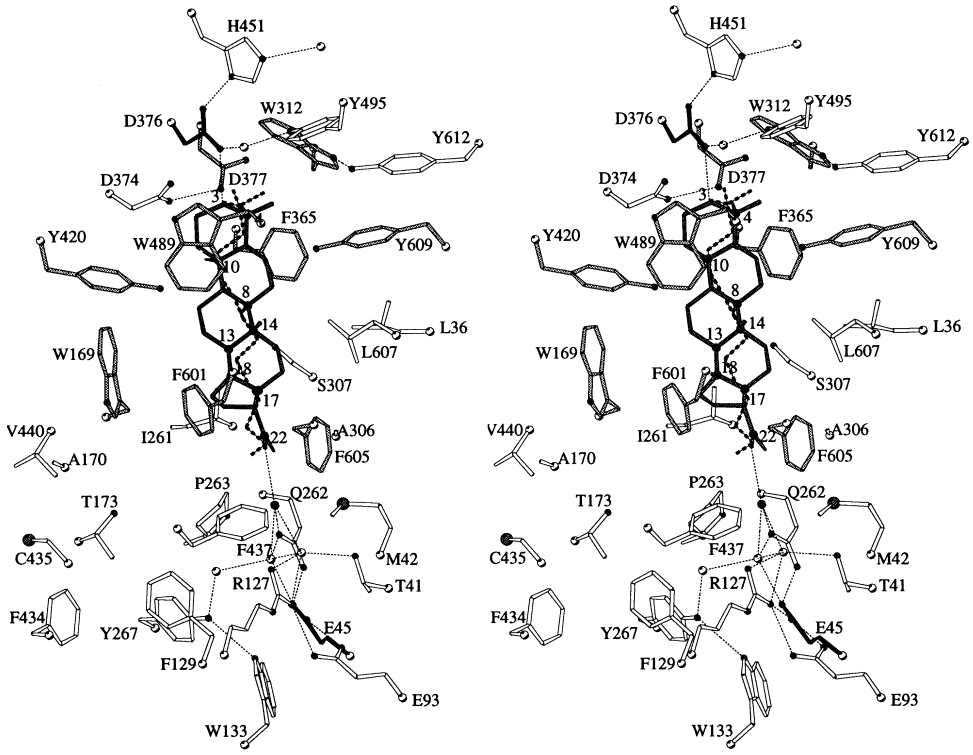

Figure 20. Stereoview of the active site of *A. acidocaldarius* squalene–hopene cyclase with the inhibitor LDAO (dotted) and a modeled hopene (gray). Hopene was modeled in the wild-type structure,[63] whereas the water molecules (open circles) and the neighboring amino acids are from the high-resolution structure of mutant Asp376Cys.[64] Asp376 and Glu45 in the polar patches at the top and bottom of the cavity are shown in black. The expected cation positions are depicted as black circles on the hopene model and the suggested position for the reactive water leading to diplopterol is depicted next to residue Gln262. Residues that are suggested or implicated for cation stabilization are highlighted in gray.

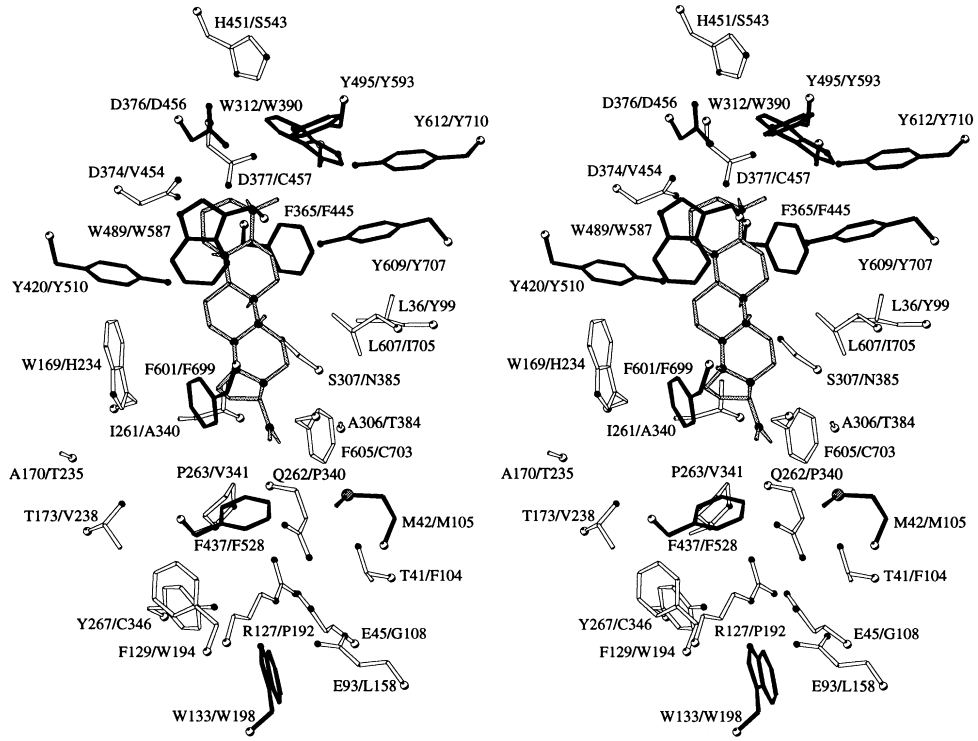

Figure 21. Alignment of *A. acidocaldarius* squalene–hopene cyclase and *S. cerevisiae* oxidosqualene–lanosterol cyclase mapped onto the active-site structure of squalene–hopene cyclase. The residue numbers on the right correspond to the squalene–hopene cyclase and those on the left to oxidosqualene–lanosterol cyclase. Identical residues are depicted in black. The hopene model (gray) and the expected cation positions (black dots) are taken from Figure 20. The alignment was taken from a multiple sequence alignment generated with the program CLUSTAL.[105] The figure suggests a gradient in homology of active-site residues ranging from low homology at the bottom of the active-site cavity (around Glu45) to higher homology at the top of the cavity (around Asp376).

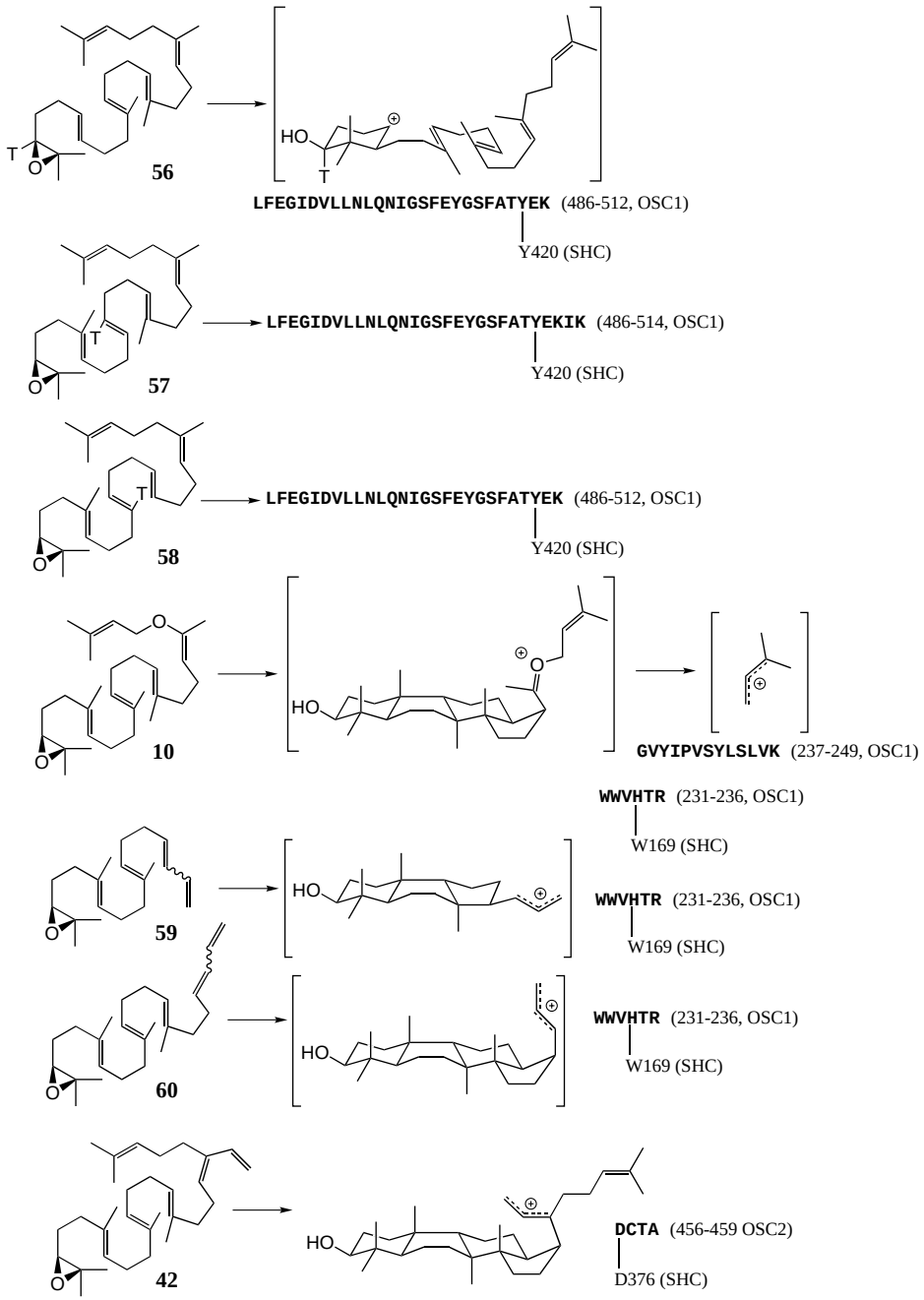

Figure 22. Labeling of oxidosqualene cyclases with suicide inhibitors.[17, 18, 41] OSC1 = Oxidosqualene cyclase from *S. cerevisiae*, OSC2 = rat liver oxidosqualene cyclase, SHC = squalene – hopene cyclase from *A. acidocaldarius.*

4. The Enzymatic Mechanism: A Unified View

A comparison of the chemical studies on uncatalyzed versus cyclase-catalyzed processes reveals that the elementary chemical steps required for triterpene formation can take place in nonenzymatic reactions following predictable chemical principles. The roles of the cyclase enzymes are, therefore: 1) Presenting a Brønsted acid of sufficient strength to initiate cyclization; 2) enforcing stereochemistry of the transition state wherever a nonchair-like conformation is required; 3) shielding cationic intermediates from premature quenching by enzyme nucleophiles or by water long enough for cyclizations and rearrangements to proceed along one controlled pathway; and 4) accelerating the reaction by stabilizing carbocations with an electron-rich environment. Below we present a unified mechanism that is consistent with the present body of chemical and structural findings (Schemes 1 and 2).

4.1. Suitability of the Cyclase Structure as a Scaffold for Mechanistic Interpretation

The crystal structure of *A. acidocaldarius* squalene – hopene cyclase was determined at 2.8 Å resolution (wild-type)[63] and at 2.0 Å resolution (inactive mutant Asp376Cys).[64] The estimated coordinate errors of about 0.4 and 0.2 Å, respectively, for these structures allow for the identification of hydrogen-bonding networks and the localization of tightly bound water molecules. In light of the current absence of a high-resolution structure of a triterpene cyclase complexed with a transition state analogue, hopene has been tentatively modeled into the active site of squalene – hopene cyclase following the substrate orientation discussed in Section 3.3.[64]

After manual placement of a hopene model in the active site, 36 binding modes were generated by rotation around the C3–C17 axis of hopene in 10° increments. The van der Waals energy of all resulting positions was minimized computationally using XPLOR.[86] No protein movement was permitted

also results in significantly increased production of **47** in contradiction with the model proposed in Figure 24.[38] Mutants Trp489Val and Trp489Leu, however, possess no activity,[38] while Trp489Ala has decreased catalytic activity without altered product distribution.[70] Since the placement of Trp489 within the structure (Figure 20) suggests that this residue is not well positioned to interact with cation **67** (Figure 15), these results may be explained if nonisosteric replacements of Trp489 displace the C19 cation (squalene numbering) away from stabilizing aromatic residues in the lower part of the active-site cavity, such as Trp169 and Phe601 (see below).

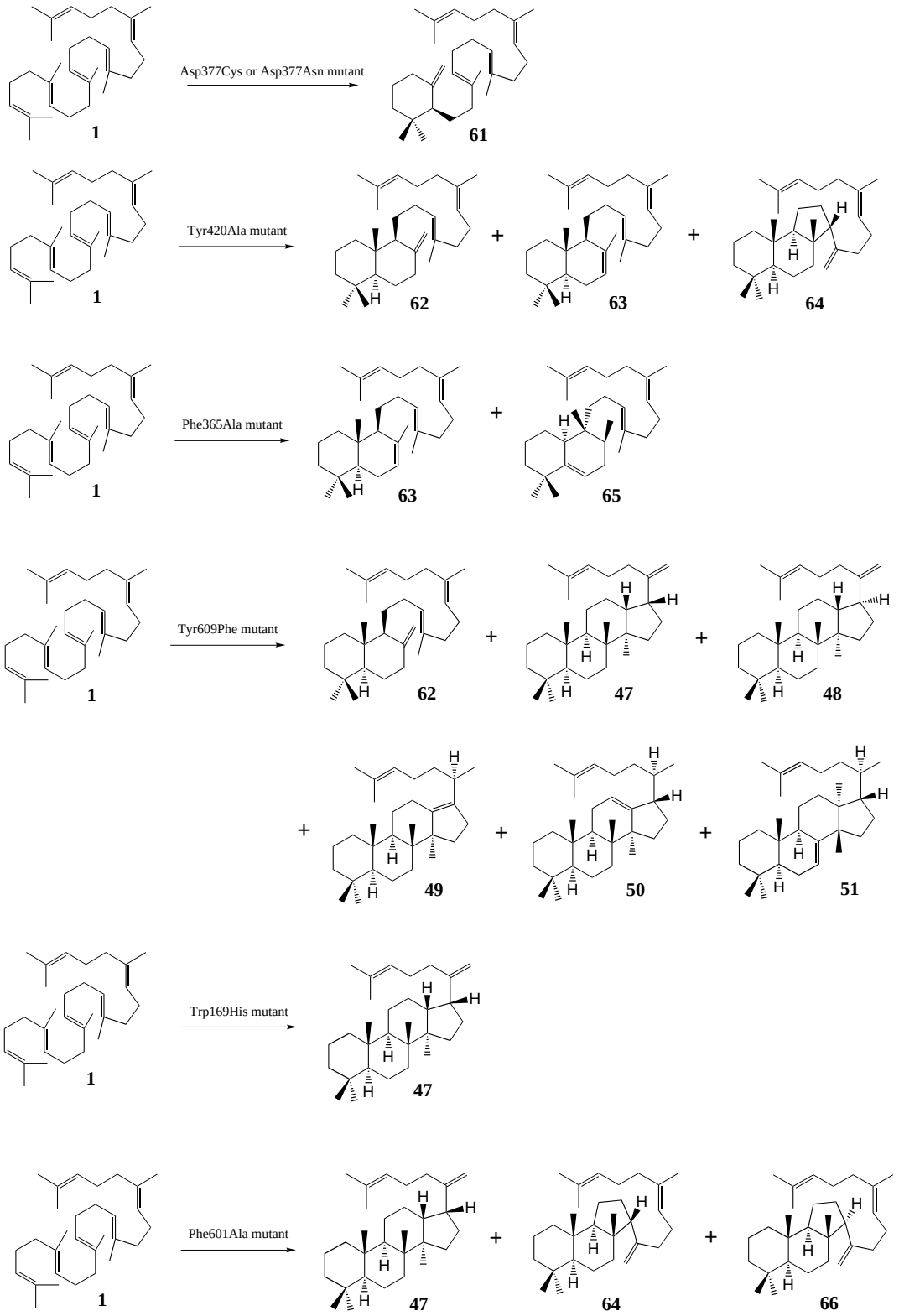

Figure 23. Partially cyclized products resulting from the incubation of squalene with squalene–hopene cyclases bearing mutations at putative cation-stabilizing residues.[37, 38, 70–73]

during the minimization and hopene was treated as a rigid body. All low-energy binding conformations clustered tightly around the most favorable one shown in Figure 20. A second minimization round allowed for rotation around the C21−C22 bond of hopene but resulted in no significant changes. The resulting model shows no residual clashes between protein and hopene atoms and serves as a starting basis for further mechanistic discussion. The A ring of the modeled hopene molecule is in good agreement with the binding mode of the observed inhibitor LDAO (Figure 20), with its C3 atom at

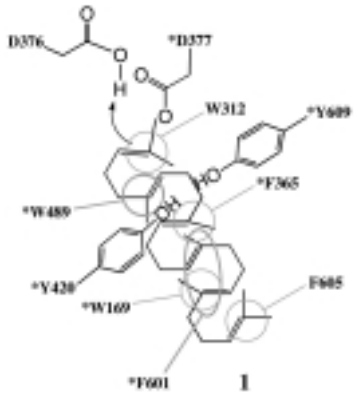

Figure 24. Proposed cation-stabilization interactions during squalene cyclization. Interactions supported by mutagenesis data are marked with an asterisk (see also Figure 20).

this preliminary working model may reflect the approximate location of the initiation and termination steps of the reaction.[64]

4.2. Initiation

4.2.1. Squalene–Hopene Cyclase

The following mechanism has been proposed for the initial protonation.[63, 64] The catalytic acid Asp376 lies 3.0 Å from the C3 atom of the modeled hopene, in agreement with the expected geometry for protonation (Figures 20 and 25). Asp376 and His451 are hydrogen bonded at 2.8 Å distance. Since a strong Brønsted acid is required for olefin protonation, it is likely that both residues are protonated prior to initiation. An additional hydrogen bond to an ordered water molecule, which connects Asp376 to the side chain hydroxyl of Tyr495, may further enhance the acidity of Asp376 (Figures 20 and 25); the lowered activity of the Tyr495Phe mutant[73] is consistent with this hypothesis. A net negative charge on the tightly hydrogen-bonded Asp374:Asp377 pair (2.6 Å distance) has been suggested to accommodate the positive charge on the Asp376:His451 pair, located in the otherwise uncharged core of the protein structure, prior to proton transfer. Interestingly, Asp376 is clearly oriented in the enzyme crystal structure to donate its *anti* proton to squalene. Consistent with the evolution of squalene–hopene cyclase to provide a strong acid for olefin protonation, carboxylic acid protons in the *anti* conformation have been estimated to be 10^4 times more acidic than those in the *syn* conformation.[87] The Asp376:His451 pair loses its charge following proton transfer to squalene, leaving the remaining negative charge on the Asp374:Asp377 pair for stabilization of the initial cationic intermediates.[63] In support of this hypothesis, mutation of Asp377 to Cys or Asn leads to the formation of monocyclic product **61** (Figure 23), suggesting that this residue stabilizes the C10 cation during cyclization.[69] Lowered catalytic rates upon mutation of His451 and Asp374 further support their roles in the initial protonation.[68, 69] The reprotonation of Asp376

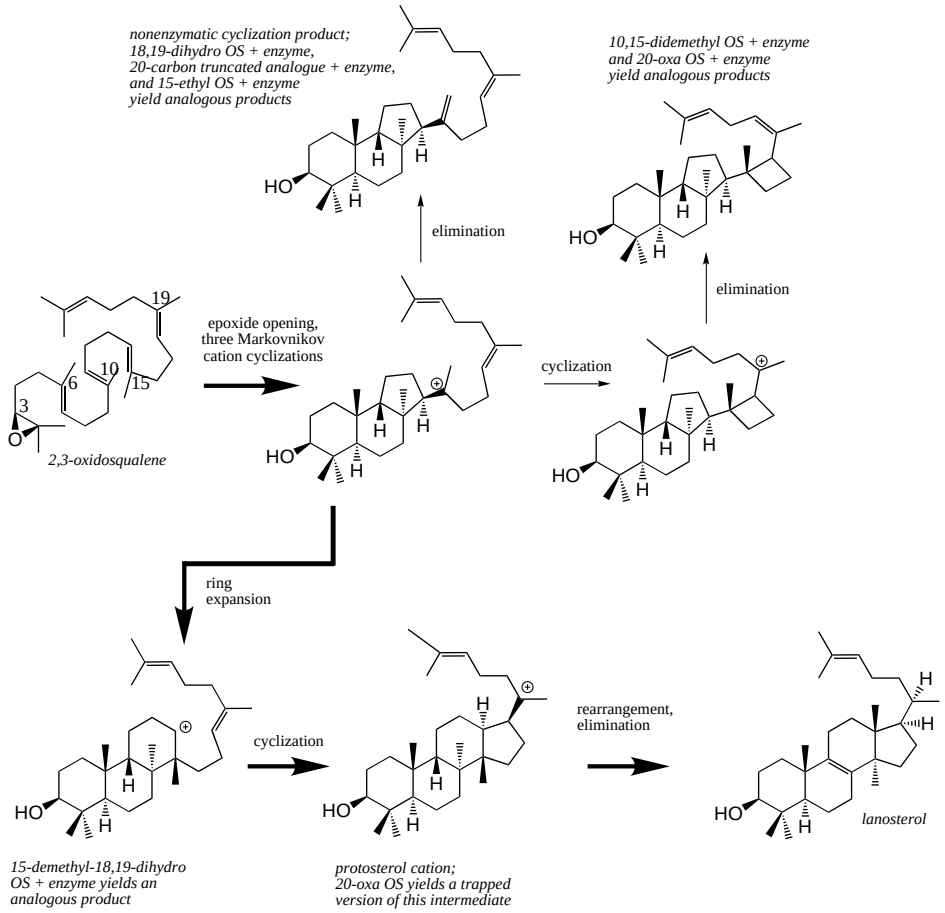

Scheme 1. The enzyme-catalyzed cyclization of oxidosqualene into lanosterol. This appears to occur through epoxide protonation by an acidic group of the enzyme which leads to epoxide opening; this is concerted with one, two, or three Markovnikov cation cyclizations to a tricyclic intermediate. The ring widening of the C ring and the Markovnikov cyclization of the intermediate complete the protosterol skeleton which is converted into lanosterol by a series of hydride and methyl group transfers. Products from an elimination, a direct cyclization, or a ring expansion of the key intermediate are obtained from enzymatic reactions with a number of substrate analogues. OS = oxidosqualene.

3.0 Å distance from the carbonyl oxygen of Asp376. The lower part of the model places the C22–C29 double bond of hopene, which is uniquely formed by squalene–hopene cyclases, in proximity to Phe605, a residue uniquely conserved among squalene–hopene cyclases. These findings suggest that

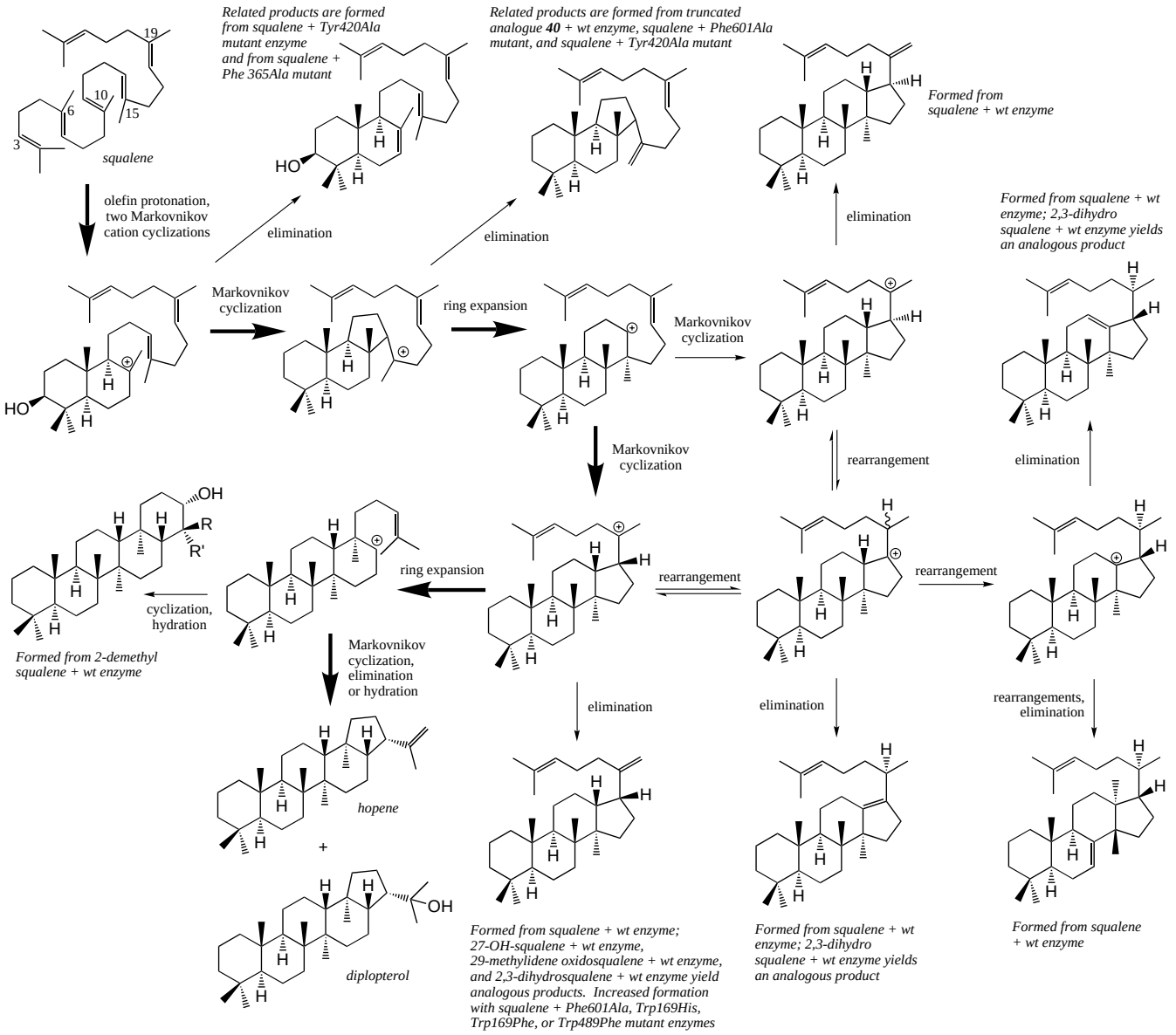

Scheme 2. The enzyme-catalyzed cyclization of squalene to hopene. An olefin protonation caused by an acidic enzyme group begins the transformation. This protonation can be concerted with one or two Markovnikov cation cyclizations. The C and D rings probably arise from ring closure of the five-membered Markovnikov cations, which for their parts allow ring expansion. A final Markovnikov cyclization completes the hopene skeleton. Products have been isolated from premature cyclizations or eliminations for almost all of the putative intermediates. The products can be side products from the natural reaction of squalene by the wild-type enzyme, from the transformation of substrate analogues, or from the transformation of squalene with a squalene – hopene cyclase mutant. wt = wild-type.

can occur through Tyr 495-OH, which in turn can transfer protons from disordered water in the solvent-accessible upper cavity of squalene – hopene cyclase (Figures 17 and 25).[64] This conclusion is consistent with the significant loss of catalytic activity arising from replacement of Tyr 495 with Phe.[73]

4.2.2. Oxidosqualene – Lanosterol Cyclase

While a hydrogen-bonded Asp 456:His 146 pair has been suggested to serve as the catalytic acid for the initial protonation in *S. cerevisiae* oxidosqualene – lanosterol cyclase,[18] the structural data on *A. acidocaldarius* squalene – hopene cyclase, in combination with a sequence alignment, suggest that His 146 is in domain 2 of the enzyme and is therefore distal from the putative catalytic acid Asp 456. Since epoxides are more readily protonated than olefins, an isolated aspartic acid may suffice as the catalytic acid for the oxidosqualene cyclases. This view is also consistent with the fact that the hydrogen-bonded Asp 374:Asp 377 pair proposed to compensate the charge on the catalytic Asp:His pair in squalene – hopene cyclase is conserved within the squalene cyclase family but is not present among oxidosqualene cyclases.[63]

4.3. Ring Formation

The chemical and theoretical studies described above indicate that A- and, possibly, B-ring formation are concerted with the initial epoxide or olefin protonation and probably

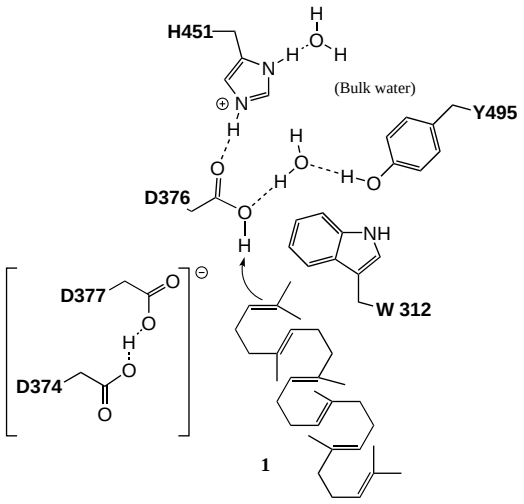

Figure 25. Proposed mechanism for the initial protonation during squalene cyclization.[64]

facilitate the initiation of the cyclization cascade. Based on the structure of squalene–hopene cyclase (Figure 20), it has been proposed that Trp312, Trp489, and Phe365 stabilize the carbocations forming at C2, C6, and C10 of squalene (C4, C10, and C8 according to hopene numbering, see Figure 24), respectively.[64] Residues Tyr420, Tyr609, and Tyr612 are oriented with their hydroxyl groups pointing towards the active-site cavity and may provide additional negative electrostatic potential during early cyclization events.[64, 78] Indeed, mutation of Tyr612 to Phe results in a significant loss of catalytic activity.[73]

The increased formation of bicyclic products **62** and **63** resulting from the Tyr420Ala squalene–hopene cyclase mutant agrees with such a role for Tyr420 (Figures 23 and 24).[71] Similarly, the formation of bicyclic product **62** arising from mutation of Tyr609 to Phe also supports the above model.[73] The production of compounds **63** and **65** by mutant Phe365Ala (Figure 23) additionally points towards a cation–π interaction between Phe365 and the C8 cation (hopene numbering, Figure 20).[71] Consistent with these suggestions, Trp312, Trp489, Phe365, Tyr609, and Tyr612 are conserved among squalene and oxidosqualene cyclases. These amino acids, thus, provide a hydrophobic, non-nucleophilic, and electron-dense environment for promoting the initial cyclization steps (see above).

It is likely that C-ring formation in the case of oxidosqualene cyclase proceeds by a five-membered cyclization followed by a ring expansion (see above). Perhaps this five-membered intermediate is kinetically favored over the six-membered alternative for Markovnikov reasons, while subsequent cyclization steps thermodynamically favor products with a six-membered C ring. Indeed, further Markovnikov cyclization of the 6-6-5 cation would lead to a strained 6-6-5-4 product (see Scheme 1). In analogy to the oxidosqualene cyclases, it is reasonable to expect a ring-widening step in the C-ring formation of squalene–hopene cyclase as the kinetically favored pathway. Demonstrating the possibility of such a cyclization pathway within squalene–hopene cyclase, the Tyr420Ala mutant of this enzyme forms 6-6-5 triene **64** as a minor product,[71] and 6-6-5 products **64** and **66** were recently isolated from the Phe601Ala mutant of squalene–hopene cyclase[37] (Figure 23). Finally, the enzyme has been shown to process truncated alcohol **40** into a 6-6-5 product consistent with trapping of the Markovnikov cation generated from five-membered C-ring closure (Figure 13).[37]

The isolation of varying amounts of 6-6-6-5 products in the reaction of wild-type and mutant squalene–hopene cyclases points strongly toward a five-membered closure and ring expansion for D-ring formation catalyzed by squalene–hopene cyclase.[38, 42, 70] A five-membered D-ring intermediate may be favored by 1,3-diaxial repulsion between the C15 and C19 methyl groups of squalene in the six-membered D-ring alternative; this difference, however, does not apply to hopene C-ring formation. Based on the data of Abe et al.[37, 38] and Merkofer et al.,[70] we propose that Trp169 and Phe601 stabilize cation **67** (Figures 15 and 20) which arises from five-membered D-ring cyclization (see above). The hopene model, derived by energy minimization prior to recent mutagenesis results, gratifyingly places Trp169 and Phe601 in close proximity to the expected positions of the C19 cation (C18 in hopene numbering) in **67** (Figures 20 and 24).[64] Taken together, these observations suggest that a 6-6-6-5 tetracycle is an on-pathway intermediate of hopene cyclization rather than simply a side product of the reaction.

Phe605 seems well positioned to stabilize the terminal cation resulting from E-ring formation in squalene–hopene cyclase (Figure 20).[64] This hypothesis is supported by the conservation of Phe605 among all known squalene cyclases (all of which form pentacyclic products) as well as the absence of this residue in the oxidosqualene–lanosterol cyclases (all of which form only four rings).[64]

Assuming that the C20 protosterol cation formed by oxidosqualene–lanosterol cyclases binds to the conserved aromatic residues in a manner similar to that of the 6-6-6-5 intermediate formed by squalene–hopene cyclase, Trp232 and/or His234, as well as Phe699, may serve to stabilize the C20 protosterol cation in the *S. cerevisiae* oxidosqualene cyclase (Figure 21). Among these residues, Trp232 is conserved within the oxidosqualene cyclases only, whereas Phe699 corresponds to Phe601 of squalene–hopene cyclase and is, therefore, conserved among both classes of enzymes. This view is consistent with the enzyme-labeling and mutagenesis experiments on the *S. cerevisiae* cyclase described above.[18]

4.4. Rearrangement and Elimination

No methyl or hydride rearrangement occurs on the pathway to hopene, although the proposed 6-6-6-5 intermediate **67** (Figure 20) undergoes rearrangements to yield small amounts of minor products.[42] Termination occurs by elimination to the main product hopene (80%) or by addition of water to diplopterol (20%).[44] In the structure of squalene–hopene cyclase determined at a resolution of 2.0 Å, a network of well-defined water molecules exists in the lower part of the active-site cavity (Figure 20).[64] It has been proposed that these bound waters are polarized by residues in the extended

hydrogen-bonding network around Glu 45 at the bottom of the active-site cavity.[64] The position of Glu 45 within the squalene–hopene cyclase structure together with its conservation among the squalene cyclases suggest that a polarized water molecule may abstract a proton or attack the E-ring cation, leading to hopene or diplopterol formation. All partially cyclized products isolated from the action of squalene–hopene cyclases on a wide variety of substrate analogues contain olefins resulting from proton elimination, rather than hydroxyl groups resulting from cation hydration (see above). This finding suggests that the water network around Glu 45 may be the only location in which active-site water is available for cation quenching.

Substrate analogue studies with the oxidosqualene cyclases described above suggest that the enzyme's role during rearrangement is most likely to simply shield intermediate carbocations from addition of water or elimination by base, thereby allowing the hydride and methyl group migrations to proceed down a thermodynamically favorable and kinetically facile cascade. A homology-based structural alignment of *S. cerevisiae* oxidosqualene cyclase and *A. acidocaldarius* squalene–hopene cyclase (Figure 21) suggests that His 234, an essential and conserved residue within the oxidosqualene–lanosterol cyclases,[18] may be well positioned to serve as the catalytic base in the oxidosqualene cyclases.

5. Future Directions

5.1. Structural Biology

The first structural elucidation of a triterpene cyclase, in conjunction with the wealth of recent chemical and biochemical data, has advanced our understanding of the mechanism of triterpene cyclization to a new level. An in-depth and detailed understanding of the roles of cyclases in substrate prefolding and cation stabilization clearly requires the determination of additional triterpene cyclase structures. Given the large quantity of chemical data that is now available for the oxidosqualene–lanosterol cyclases together with their potential medical importance, the structural determination of an oxidosqualene cyclase is a major priority in this field. These efforts will, hopefully, be assisted by the rapid development of new techniques in membrane protein expression and crystallization.[88, 89] While the human and *Candida albicans* oxidosqualene cyclases are highly attractive targets for the development of anticholesteremic and antifungal drugs, our understanding of the enzymatic mechanism would also be facilitated by the structure of more tractable bacterial or fungal cyclases.

5.2. Structure-Based Mutagenesis

Recent successes in structure-based mutagenesis and the careful analysis of resulting altered product distributions have added greatly to our understanding of the mechanism of triterpene cyclases. The characterization of further mutants will undoubtedly continue to enhance our understanding of these enzymes. For clarity, squalene–hopene cyclase residue numbering will be used throughout this section, although analogous experiments on oxidosqualene cyclases are also relevant.

Mutations Leu 36 Tyr and Leu 607 Ile for squalene–hopene cyclase and the corresponding mutations Tyr 99 Leu and Ile 705 Leu for oxidosqualene–lanosterol cyclase may provide insight into the role of these residues in the determination of B-ring configuration or in ring widening during C-ring formation. The repeated observation of multiple partially cyclized products arising from many of the site-directed mutants described above reflects the general problem of separating specific π-cation interactions from simple steric effects that may arise from displacement of the forming product in the active-site cavity or from subtle changes in the structure of the active site. This problem is particularly evident in the partially contradictory reports of Sato et al.[38] and Merkofer et al.[70] related to D-ring formation in squalene–hopene cyclase. Isosteric replacements using unnatural amino acid mutagenesis[90] may resolve such contradictions. Replacement of Trp 489, Phe 601, and Trp 169 with fluorinated analogues of these amino acids would provide series of relatively isosteric side chains with varying levels of electron richness and, thus, varying abilities to stabilize cations. A correlation between electron richness and product distributions arising from trapping of putative 6-6-6-5 intermediates would support specific π-cation interactions. The need to develop in vitro expression of these enzymes in the presence of lipids and to analyze very minor products arising from these mutant enzymes, together with the low turnover number of squalene–hopene cyclase ($0.3\ s^{-1}$), however, will make this a challenging endeavor. Generation of a monomeric squalene–hopene cyclase by mutations in the suggested dimer interface may clarify whether dimer formation is required for enzymatic activity and membrane binding.

5.3. Directed Evolution

The relaxed substrate and product specificities of mutant squalene–hopene cyclases point to the possibility of generating novel triterpenes by the directed evolution of these enzymes.[91, 92] In support of this hypothesis, an Ile 481 Val mutant oxidosqualene–cycloartenol cyclase, which can produce lanosterol, was recently isolated by spontaneous mutation and genetic selection in a yeast strain unable to produce lanosterol.[93] A terpene-cyclase catalytic antibody that catalyzes the cyclization of an unnatural sesquiterpene to a series of unsaturated *trans*-decalins[94] also structurally mimics the active site of a natural sesquiterpene cyclase.[95–97] Even though no catalytic antibody with triterpene cyclase activity has been described at present,[98] the development of methods to generate such catalysts may open new routes to unnatural triterpenes.[99, 100]

Since many squalene cyclases are known to accept oxidosqualene as a substrate,[9] it may be possible to apply directed-evolution strategies to squalene–hopene (or other non-lanosterol forming) cyclases.[101, 102] The oxidosqualene–lanosterol cyclase deficient yeast strain *ERG7* provides an

opportunity to select in vivo for lanosterol formation.[53] The structure of an evolved squalene–hopene cyclase mutant capable of lanosterol formation may yield valuable information on the structural requirements for different transition state geometries and backbone rearrangements unbiased by natural evolutionary drift. More generally, the generation and use of mutant organisms known to be deficient in the production of other essential triterpenes provides the opportunity to apply genetic selections towards the artificial evolution of cyclase enzymes with new product specificities. The rigorous analysis of mutations responsible for altered product specificities may provide important insights into the roles of residues both near and distant from the active site in defining the course of these mechanistically complex yet extremely elegant enzyme-catalyzed cyclizations.

This work was supported by the National Institutes of Health (Grant GM-34167 to E.J.C), the Sonderforschungsbereich 388 (K.U.W. and G.E.S), and a postdoctoral fellowship from BASF and the Deutsche Studienstiftung (K.U.W).

Received: November 18, 1999 [A 371]

[1] R. B. Woodward, K. Bloch, *J. Am. Chem. Soc.* **1953**, *75*, 2023–2024.
[2] G. Stork, A. W. Burgstahler, *J. Am. Chem. Soc.* **1955**, *77*, 5068–5077.
[3] A. Eschenmoser, L. Ruzika, O. Jeger, D. Arigoni, *Helv. Chim. Acta.* **1955**, *38*, 1890–1904.
[4] R. K. Maugdal, T. T. Tchen, K. Bloch, *J. Am. Chem. Soc.* **1958**, *80*, 2589–2590.
[5] J. W. Cornforth, R. H. Cornforth, C. Donninger, G. Popjak, Y. Shimizu, S. Ichii, E. Forchielli, E. Caspi, *J. Am. Chem. Soc.* **1965**, *87*, 3224–3228.
[6] E. J. Corey, W. E. Russey, P. R. Ortiz de Montellano, *J. Am. Chem. Soc.* **1966**, *88*, 4750–4751.
[7] E. J. Corey, W. E. Russey, *J. Am. Chem. Soc.* **1966**, *88*, 4751–4752.
[8] E. E. van Tamelen, J. D. Willett, R. B. Clayton, K. E. Lord, *J. Am. Chem. Soc.* **1966**, *88*, 4752–4754.
[9] I. Abe, M. Rohmer, G. D. Prestwich, *Chem. Rev.* **1993**, *93*, 2189–2206.
[10] E. J. Corey, D. D. Staas, *J. Am. Chem. Soc.* **1998**, *120*, 3526–3527.
[11] K. Poralla in *Comprehensive natural products chemistry*, *Vol. 5* (Eds.: D. Barton, K. Nakashini, O. Meth-Cohn), Pergamon, Oxford, **1999**, pp. 299–319.
[12] C. Jenson, W. L. Jorgensen, *J. Am. Chem. Soc.* **1997**, *119*, 10846–10854.
[13] E. J. Corey, S. C. Virgil, H. Cheng, C. H. Baker, S. P. T. Matsuda, V. Singh, S. Sarshar, *J. Am. Chem. Soc.* **1995**, *117*, 11819–11820.
[14] E. J. Corey, S. C. Virgil, S. Sarshar, *J. Am. Chem. Soc.* **1991**, *113*, 8171–8172.
[15] B. Robustell, I. Abe, G. D. Prestwich, *Tetrahedron Lett.* **1998**, *39*, 957–960.
[16] B. Robustell, I. Abe, G. D. Prestwich, *Tetrahedron Lett.* **1998**, *39*, 9385–9388.
[17] E. J. Corey, H. Cheng, C. H. Baker, S. P. T. Matsuda, D. Li, X. Song, *J. Am. Chem. Soc.* **1997**, *119*, 1277–1288.
[18] E. J. Corey, H. Cheng, C. H. Baker, S. P. T. Matsuda, D. Li, X. Song, *J. Am. Chem. Soc.* **1997**, *119*, 1289–1296.
[19] E. E. van Tamelen, D. R. James, *J. Am. Chem. Soc.* **1977**, *99*, 950–952.
[20] E. J. Corey, K. Lin, M. J. Jautelat, *J. Am. Chem. Soc.* **1968**, *90*, 2724–2726.
[21] L. O. Crosby, E. E. van Tamelen, R. B. Clayton, *J. Chem. Soc. Chem. Commun.* **1969**, 532–533.
[22] J. C. Medina, K. S. Kyler, *J. Am. Chem. Soc.* **1988**, *110*, 4818–4821.
[23] X.-y. Xiao, S. E. Sen, G. D. Prestwich, *Tetrahedron Lett.* **1990**, *31*, 2097–2100.
[24] D. Gao, Y.-K. Pan, K. Byun, J. Gao, *J. Am. Chem. Soc.* **1998**, *120*, 4045–4046.
[25] T. Hoshino, Y. Sakai, *Chem. Commun.* **1998**, 1591–1592.
[26] E. E. van Tamelen, K. B. Sharpless, R. Hanzlik, R. B. Clayton, A. L. Burlingame, P. C. Wszolek, *J. Am. Chem. Soc.* **1967**, *89*, 7150–7151.
[27] E. J. Corey, H. Cheng, *Tetrahedron Lett.* **1996**, *37*, 2709–2712.
[28] E. J. Corey, S. C. Virgil, D. R. Liu, S. Sarshar, *J. Am. Chem. Soc.* **1992**, *114*, 1524–1525.
[29] J. W. Cornforth, *Angew. Chem.* **1968**, *80*, 977–985; *Angew. Chem. Int. Ed. Engl.* **1968**, *7*, 903–911.
[30] W. R. Nes, T. E. Varkey, K. Krevitz, *J. Am. Chem. Soc.* **1977**, *99*, 260–262.
[31] E. J. Corey, S. C. Virgil, *J. Am. Chem. Soc.* **1991**, *113*, 4025–4026.
[32] E. J. Corey, D. C. Daley, H. Cheng, *Tetrahedron Lett.* **1996**, *37*, 3287–3290.
[33] E. J. Corey, S. C. Virgil, *J. Am. Chem. Soc.* **1990**, *112*, 6429–6431.
[34] E. E. van Tamelen, J. W. Murphy, *J. Am. Chem. Soc.* **1970**, *92*, 7204–7206.
[35] E. E. van Tamelen, J. H. Freed, *J. Am. Chem. Soc.* **1970**, *92*, 7206–7207.
[36] E. E. van Tamelen, J. Willet, M. Schwartz, R. Nadeau, *J. Am. Chem. Soc.* **1966**, *88*, 5937–5938.
[37] T. Hoshino, M. Kouda, T. Abe, S. Ohashi, *Biosci. Biotechnol. Biochem.* **1999**, *63*, 2038–2041.
[38] T. Sato, T. Abe, T. Hoshino, *Chem. Commun.* **1998**, 2617–2618.
[39] I. Abe, T. Y. Dang, Y. F. Zheng, B. A. Madden, C. Feil, K. Poralla, G. D. Prestwich, *J. Am. Chem. Soc.* **1997**, *119*, 11333–11334.
[40] I. Abe, M. Rohmer, *J. Chem. Soc. Chem. Commun.* **1991**, 902–903.
[41] I. Abe, M. Rohmer, *J. Chem. Soc. Perkin Trans. 1* **1994**, 783–791.
[42] C. Pale-Grosdemange, C. Feil, M. Rohmer, K. Poralla, *Angew. Chem.* **1998**, *110*, 2355–2358; *Angew. Chem. Int. Ed.* **1998**, *37*, 2237–2240.
[43] T. Hoshino, T. Kondo, *Chem. Commun.* **1999**, 731–732.
[44] B. Seckler, K. Poralla, *Biochim. Biophys. Acta* **1986**, *881*, 356–363.
[45] C. H. Baker, S. P. T. Matsuda, D. R. Liu, E. J. Corey, *Biochem. Biophys. Res. Commun.* **1995**, *213*, 154–160.
[46] I. Abe, M. Bai, X.-y. Xiao, G. D. Prestwich, *Biochem. Biophys. Res. Commun.* **1992**, *187*, 32–38.
[47] M. Kusano, M. Shibuya, U. Sankawa, Y. Ebizuka, *Biol. Pharm. Bull.* **1995**, *18*, 195–197.
[48] C. H. Buntel, J. H. Griffin, *J. Am. Chem. Soc.* **1992**, *114*, 9711–9713.
[49] C. A. Roessner, C. Min, S. H. Hardin, L. W. Harris-Haller, J. C. McCollum, A. I. Scott, *Gene* **1993**, *127*, 149–150.
[50] Z. Shi, C. J. Buntel, J. H. Griffin, *Proc. Natl. Acad. Sci. USA* **1994**, *91*, 7370–7374.
[51] E. J. Corey, S. P. T. Matsuda, B. Bartel, *Proc. Natl. Acad. Sci. USA* **1994**, *91*, 2211–2215.
[52] E. J. Corey, S. P. T. Matsuda, C. H. Baker, A. Y. Ting, H. Cheng, *Biochem. Biophys. Res. Commun.* **1996**, *219*, 327–331.
[53] E. J. Corey, S. P. T. Matsuda, B. Bartel, *Proc. Natl. Acad. Sci. USA* **1993**, *90*, 11628–11632.
[54] T. Kushiro, M. Shibuya, Y. Ebizuka, *Eur. J. Biochem.* **1998**, *256*, 238–244.
[55] D. Ochs, C. Kaletta, K. D. Entian, A. Beck-Sickinger, K. Poralla, *J. Bacteriol.* **1992**, *174*, 298–302.
[56] I. G. Reipen, K. Poralla, H. Sahm, G. A. Sprenger, *Microbiology* **1995**, *141*, 155–161.
[57] M. Perzl, P. Müller, K. Poralla, E. L. Kannenberg, *Microbiology* **1997**, *143*, 1235–1242.
[58] A. Tippelt, L. Jahnke, K. Poralla, *Biochim. Biophys. Acta.* **1998**, *1391*, 223–232.
[59] C. Freiberg, R. Fellay, A. Bairoch, W. J. Broughton, A. Rosenthal, X. Perret, *Nature* **1997**, *387*, 394–401.
[60] T. Kaneko, S. Sato, H. Kotani, A. Tanaka, E. Asamizu, Y. Nakamura, N. Miyajima, M. Hirosawa, M. Sugiura, S. Sasamoto, T. Kimura, T. Hosouchi, A. Matsuno, A. Muraki, N. Nakazaki, K. Naruo, S. Okumura, S. Shimpo, C. Takeuchi, T. Wada, A. Watanabe, M. Yamada, M. Yasuda, S. Tabata, *DNA Res.* **1996**, *3*, 109–136.
[61] F. Kunst et al. (more than 100 other authors), *Nature* **1997**, *390*, 249–256.
[62] K. U. Wendt, C. Feil, A. Lenhart, K. Poralla, G. E. Schulz, *Protein Sci.* **1997**, *6*, 722–724.
[63] K. U. Wendt, K. Poralla, G. E. Schulz, *Science* **1997**, *277*, 1811–1815.

[64] K. U. Wendt, A. Lenhart, G. E. Schulz, *J. Mol. Biol.* **1999**, *286*, 175 – 187.
[65] S. Neumann, H. Simon, *Biol. Chem. Hoppe-Seyler* **1986**, *367*, 723 – 729.
[66] K. U. Wendt, G. E. Schulz, *Structure* **1998**, *6*, 127 – 133.
[67] D. Ochs, C. H. Tappe, P. Gartner, R. Kellner, K. Poralla, *Eur. J. Biochem.* **1990**, *194*, 75 – 80.
[68] C. Feil, R. Süssmuth, G. Jung, K. Poralla, *Eur. J. Biochem.* **1996**, *242*, 51 – 55.
[69] T. Sato, T. Hoshino, *Biosci. Biotechnol. Biochem.* **1999**, *63*, 2189 – 2198.
[70] T. Merkofer, C. Pale-Grosdemange, K. U. Wendt, M. Rohmer, K. Poralla, *Tetrahedron Lett.* **1999**, *40*, 2121 – 2124.
[71] C. Pale-Grosdemange, T. Merkofer, M. Rohmer, K. Poralla, *Tetrahedron Lett.* **1999**, *40*, 6009 – 6012.
[72] T. Hoshino, T. Sato, *Chem. Commun.* **1999**, 2005 – 2006.
[73] C. Füll, K. Poralla, *FEMS Microbiol. Lett.* **2000**, *183*, 221 – 224.
[74] I. Abe, G. D. Prestwich, *J. Biol. Chem.* **1994**, *269*, 802 – 804.
[75] K. Poralla, A. Hewelt, G. D. Prestwich, I. Abe, I. Reipen, G. Sprenger, *Trends Biochem. Sci.* **1994**, *19*, 157 – 158.
[76] K. Poralla, *Bioorg. Med. Chem. Lett.* **1994**, *4*, 285 – 290.
[77] W. S. Johnson, S. D. Lindell, J. Steele, *J. Am. Chem. Soc.* **1987**, *109*, 2517 – 2518.
[78] D. A. Dougherty, *Science* **1996**, *271*, 163 – 168.
[79] G. Ourisson, Y. Nakatani, *Chem. Biol.* **1994**, *1*, 11 – 23.
[80] G. Balliano, F. Viola, M. Ceruti, L. Cattel, *Arch. Biochem. Biophys.* **1992**, *293*, 122 – 129.
[81] G. Blobel, *Proc. Natl. Acad. Sci. USA* **1980**, *77*, 1496 – 1500.
[82] D. Picot, P. J. Loll, R. M. Garavito, *Nature* **1994**, *367*, 243 – 249.
[83] C. Luong, A. Miller, J. Barnett, J. Chow, C. Ramesha, M. F. Browner, *Nat. Struct. Biol.* **1996**, *3*, 927 – 933.
[84] R. G. Kurumbail, A. M. Stevens, J. K. Gierse, J. J. McDonald, R. A. Stegeman, J. Y. Pak, D. Gildehaus, J. M. Miyashiro, T. D. Penning, K. Seibert, P. C. Isakson, W. C. Stallings, *Nature* **1996**, *384*, 644 – 648.
[85] T. Y. Dang, I. Abe, Y. F. Zheng, G. D. Prestwich, *Chem. Biol.* **1999**, *6*, 333 – 341.
[86] A. T. Brünger, *Science* **1987**, *235*, 458 – 460.
[87] R. D. Gandour, *Bioorg. Chem.* **1981**, *10*, 169 – 176.
[88] A. Pautsch, J. Vogt, K. Model, C. Siebold, G. E. Schulz, *Proteins Struct. Funct. Genet.* **1999**, *34*, 167 – 172.
[89] C. Ostermeier, S. Iwata, B. Ludwig, H. Michel, *Nat. Struct. Biol.* **1995**, *2*, 842 – 846.
[90] V. W. Cornish, D. Mendel, P. G. Schultz, *Angew. Chem.* **1995**, *107*, 677 – 690; *Angew. Chem. Int. Ed. Engl.* **1995**, *34*, 621 – 633.
[91] F. H. Arnold, A. A. Volkov, *Curr. Opin. Chem. Biol.* **1999**, *3*, 54 – 59.
[92] D. R. Liu, P. G. Schultz, *Angew. Chem.* **1999**, *111*, 36 – 56; *Angew. Chem. Int. Ed.* **1999**, *38*, 36 – 54.
[93] E. A. Hart, L. Hua, L. B. Darr, W. K. Wilson, J. Pang, S. P. T. Matsuda, *J. Am. Chem. Soc.* **1999**, *121*, 9887 – 9888.
[94] J. Hasserodt, K. D. Janda, R. A. Lerner, *J. Am. Chem. Soc.* **1997**, *119*, 5993 – 5998.
[95] C. M. Paschall, J. Hasserodt, T. Jones, R. A. Lerner, K. D. Janda, D. W. Christianson, *Angew. Chem.* **1999**, *111*, 1859 – 1864; *Angew. Chem. Int. Ed.* **1999**, *38*, 1743 – 1747.
[96] C. M. Starks, K. Back, J. Chappel, J. P. Noel, *Science* **1997**, *277*, 1815 – 1820.
[97] C. A. Lesburg, J. M. Caruthers, C. M. Paschall, D. W. Christianson, *Curr. Opin. Struct. Biol.* **1998**, *8*, 695 – 703.
[98] P. G. Schultz, R. A. Lerner, *Science* **1995**, *269*, 1835 – 1842.
[99] J. Hasserodt, K. D. Janda, R. A. Lerner, *J. Am. Chem. Soc.* **1996**, *118*, 11 654 – 11 655.
[100] J. Hasserodt, K. D. Janda, R. A. Lerner, *J. Am. Chem. Soc.* **2000**, *122*, 40 – 45.
[101] W. P. C. Stemmer, *Nature* **1994**, *370*, 389 – 391.
[102] P. A. Patten, R. J. Howard, W. P. C. Stemmer, *Curr. Opin. Biotechnol.* **1997**, *8*, 724 – 733.
[103] M. L. Connolly, *J. Mol. Graph.* **1993**, *11*, 139 – 141.
[104] A. Nicholls, K. A. Sharp, B. Honig, *Proteins Struct. Funct. Genet.* **1991**, *11*, 281 – 296.
[105] J. D. Thompson, T. J. Gibson, F. Plewniak, F. Jeanmougin, D. G. Higgins, *Nucleic Acids Res.* **1997**, *25*, 4876 – 4882.